PROSES REVIEW ARTIKEL DI FME TRANSACTION

Judul: Effect of blowing flow control and front geometry towards the reduction of aerodynamic drag on vehicle models

1. Submit artikel di FME Transactions (18 November 2018)

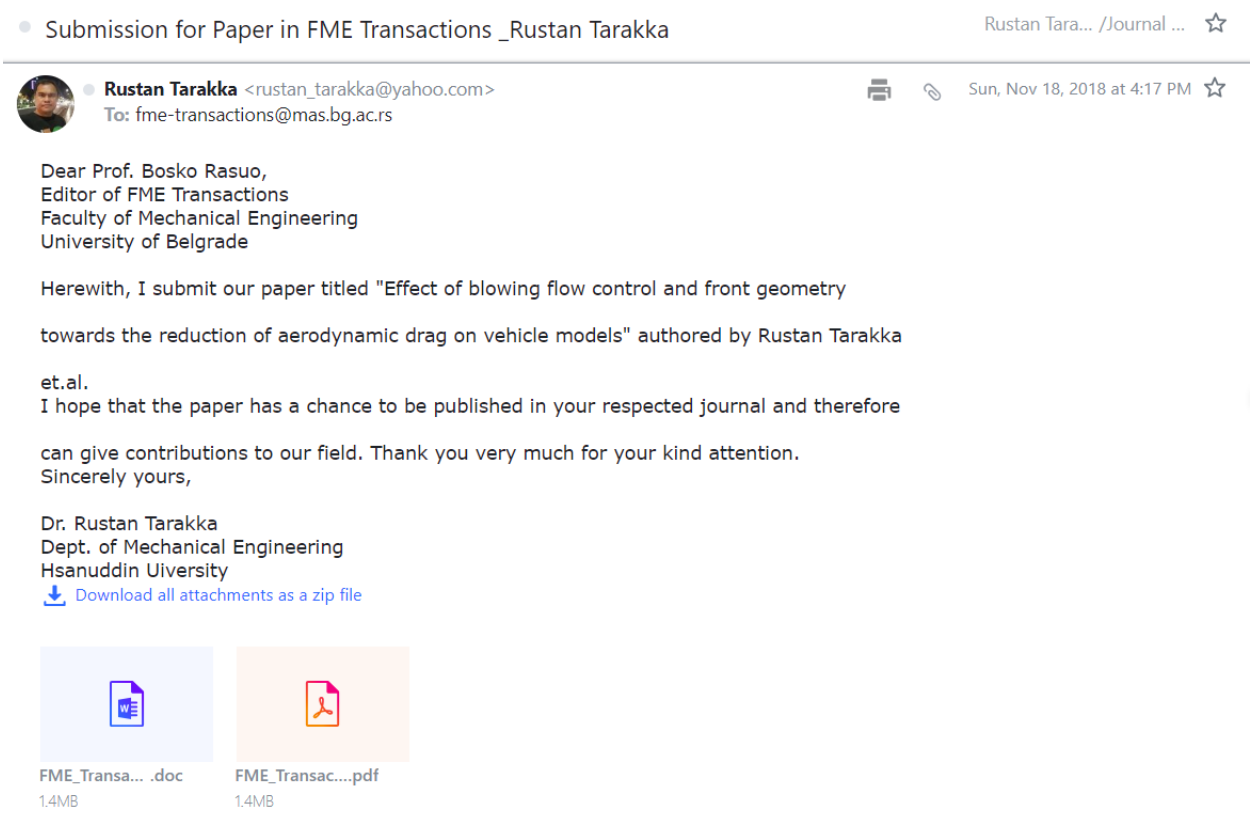

Submission for Paper in FME Transactions _Rustan Tarakka

Rustan Tara... /Journal ...

Rustan Tarakka <rustan_tarakka@yahoo.com>
To: fme-transactions@mas.bg.ac.rs

Sun, Nov 18, 2018 at 4:17 PM

Dear Prof. Bosko Rasuo,
Editor of FME Transactions
Faculty of Mechanical Engineering
University of Belgrade

Herewith, I submit our paper titled "Effect of blowing flow control and front geometry

towards the reduction of aerodynamic drag on vehicle models" authored by Rustan Tarakka

et.al.
I hope that the paper has a chance to be published in your respected journal and therefore

can give contributions to our field. Thank you very much for your kind attention.
Sincerely yours,

Dr. Rustan Tarakka
Dept. of Mechanical Engineering
Hsanuddin Uiversity

Download all attachments as a zip file

FME_Transa... .doc
1.4MB

FME_Transac....pdf
1.4MB

Effect of blowing flow control and front geometry towards the reduction of aerodynamic drag on vehicle models

Rustan Tarakka
Assistant Professor
Hasanuddin University
Department of Mechanical Engineering
Indonesia

Nasaruddin Salam
Professor
Hasanuddin University
Department of Mechanical
Indonesia

Jalaluddin
Associate Professor
Hasanuddin University
Department of Mechanical Engineering
Indonesia

Muhammad Ihsan
Lecturer
Sekolah Tinggi Teknik Baramuli
Department of Civil Engineering
Indonesia

This paper presents analyses of the effect of blowing flow control and variations on front geometry towards the reduction of aerodynamic drag on vehicle models. Blowing flow control is an alternative measure in modifying the onset of flow separation in the boundary layer on the surface of the vehicle. The modification is expected to reduce the dominating influence of the separation area on the total drag. Conducted in computational and experimental approaches, the research investigated the effect of frontal slant angle variations (θ) of 25°, 30° and 35° towards the reduction of aerodynamic drag on vehicle models on the application of blowing flow control with upstream and blowing speed of 16.7 m/s and 0.5 m/s, respectively. Load cells were used in the experimental method to validate the reduction of aerodynamic drag obtained from computational method. It is indicated that the effects of blowing flow control and variations on front geometry are significant in the increasing on pressure coefficients and the reduction of aerodynamic drag on vehicle models. The largest increase on pressure coefficients of 38.93% is indicated on the vehicle model with θ=35°, while the largest reduction of aerodynamic drag occurred on the same model with the values of 14.81 and 12.54 for computational and experimental methods, respectively.

Keywords: *active flow control, aerodynamic drag reduction, blowing, front geometry, vehicle model.*

1. INTRODUCTION

As one of the most preferred types of general vehicles, family car in the form of multi purposed van (MPV) has both advantages and drawbacks. Of the drawbacks, one typical character is the demand of relatively larger capacity engine which means larger fuel consumption than its more compact counterparts. This type also generally has the basic shape of the bluff body to maximize the space volume of the passenger compartment. In terms of aerodynamics, this form results in larger aerodynamic drag due to the occurrence of enormous flow separation in rear parts of the vehicle body creating higher energy consumption of the vehicle. The aerodynamic drag contributes about half of mechanical energy expenditures of vehicles running at average highway speed of around 55 to 60 mph [1].

Ahmed vehicle model is an extremely simplified bluff-body model frequently used as a benchmark in vehicle aerodynamics research. A number of experimental research [2-6] and numerical studies [7-12] have been performed using the Ahmed model. One of the techniques under development to reduce aerodynamic drag on vehicles and to modify the generation of flow separation in the boundary layer on the surface of the vehicle which resulted in the generation of a backflow around the vehicle is the active flow control application. Active control strategies involve the addition of energy which aims to control, either in the form of prevention or inhibiting, the occurrence of flow separation which may lead to backflow on the surface of the vehicle without changing the shape of vehicles [13].

Some active control techniques have been developed and focusing on local intervention in wall turbulence dealing with steady blowing or suction [14-22]. Krentel et.al. modeled a predictive closed-loop actuation approach for one steady blowing excitation configuration [16]. Harinaldi et al. [23] used a modified or reversed Ahmed body equipped with active flow control by blowing and found that the drag reductions achieved by computational and experimental methods were 13.92% and 11.11%. A review has also been elaborated for methods for the application of flow control on a square back car model [24]. This study aimed to analyze the effect of blowing active control incorporating the variations on front geometry towards the reduction aerodynamic drag on vehicle models. Improved reduction of aerodynamic drag can reduce flow separation which in turns will lead to energy efficiency. Comprehension of aerodynamic drag reductions and pressure coefficients are expected to improve the design method of future vehicles.

2. METHODOLOGY

The study investigates drag reduction occurring in a bluff body of van model adapted from Ahmed model, in

Received:
Correspondence to: Dr Rustan Tarakka
Department of Mechanical Engineering,
Jl. Poros Malino, Gowa, Indonesia
E-mail: rustan_tarakka@yahoo.com

which flow streams in reversed direction from the original model or in other names, reversed Ahmed model [23, 25-28]. The van model was equipped with an active control by applying blowing techniques. Reversed Ahmed body model was chosen since it is a good representation of typical forms of popular family van produced by car manufacturer. The van model was investigated in both computational method, or CFD, and experimental method.

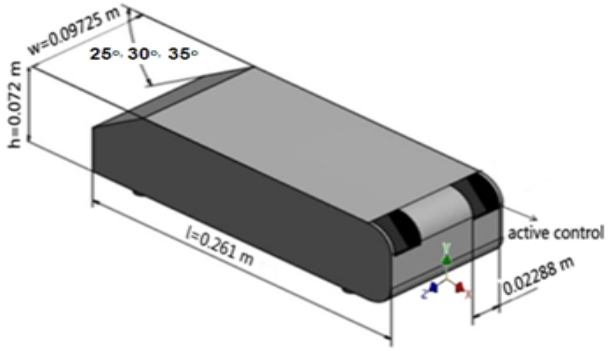

Figure 1. Reversed Ahmed body vehicle model

Figure 1 represents the basic vehicle model employed in the research with 0.25 geometric ratio to the original Ahmed body model [2]. The vehicle model geometry was defined by its length (l=0.261m), width (w =0.09725 m) and its height (h=0.072 m). In this configuration, the front part of model was inclined with slant angles (θ) of 25°, 30° and 35°relative to the horizontal reference.

The value of viscous drag force and pressure drag force F_d is denoted in the equation (1).

$$F_d = \int \tau_w \sin\theta dS + \int p \cos\theta dS \tag{1}$$

While, drag coefficient C_d is expressed in the equation (2).

$$C_d = \int \frac{\tau_w}{\frac{1}{2}\rho V_\infty^2 S} \sin\theta dS + \frac{\int Cp \cos\theta dS}{S} \tag{2}$$

where $\tau_w = \mu(du/dy)_w$ is the wall shear stress which is assessed from the velocity gradient at the wall and $C_p = (p\text{-}p_\infty)/(\rho V_\infty^2/2)$ is pressure coefficient which is assessed from pressure distribution at the wall.

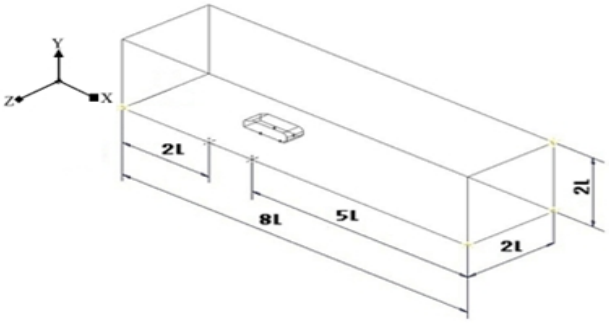

Figure 2. The 3D computational domain

The applied 3D computational domain is as shown in figure 2 denoting dimensions of length (L) = 8l, width (W) = 2l, and height (H) = 2l, where l is the length of model in x-axis. The type of meshing was tetra/hybrid element with hexcore type. Inlet velocity of 16.7 m/s is assigned as the boundary condition. Average free stream at upstream region was assumed to be in a steady state and uniform condition. The blowing speed was defined in0.5 m/s. Reynolds number corresponding to the length of the test model was at $Re=2.98x10^5$. The detailed computational conditions are given in table 1.

Table 1. Description of computational condition

Vehicle model	3D, steady state θ=25°, θ=30° andθ=35°	
Fluid	Air	
Fluid properties	Density Viscosity	1.225 kg/m^3 0.000017894 kg/m-s
Boundary condition without an active flow control	Vehicle model Pressure outlet Velocity inlet Wall	Wall Pressure outlet Velocity inlet Wall
Boundary condition with blowing flow control	Vehicle model Pressure outlet Velocity inlet Wall Blowing1 Blowing2	Wall Pressure outlet Velocity inlet Wall Velocity inlet Velocity inlet
Upstream velocity	16.7 m/s	
Blowing velocity	0.5 m/s	

The tests were conducted in a controlled low speed wind tunnel supplied with free stream air flow, testing acrylic van model with a 0.25 scale to the original Ahmed body model [2]. The van models are classified as were model without flow control and model with blowing flow control. The blowing apparatus was configured at the internal part of the body of the model where the flow separation was predicted by computational method to induce a significant drag. The blowing apparatus was operated by using a mini compressor with blowing velocity at 0.5 m/s.

The investigated parameter was the aerodynamic drag force measured by using a load cell. Prior to the main experiments, the load cell was calibrated by using a digital balance. A preliminary measurement was performed to determine the statistical uncertainty of force measurements which was predicted to range at about ± 2%.The setup for the aerodynamic drag force measurement is as shown in figure 3.

Dimensionless drag coefficient relative to drag force working on the bluff body is defined in the equation (3):

$$C_d = \frac{F_d}{\frac{1}{2}\rho V_\infty^2 S} \tag{3}$$

where, ρ is air density, V_∞ is free stream velocity, S is cross sectional area and F_d is the total drag force working on vehicle models as measured by the load cell.

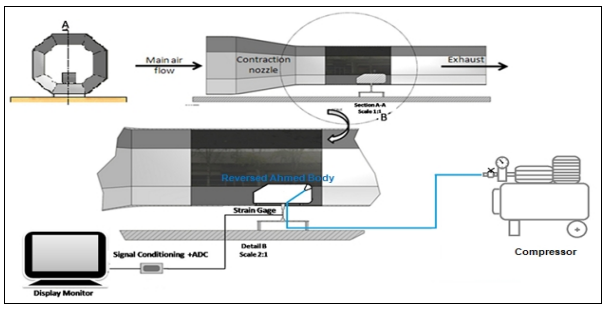

Figure 3. Experimental setup for the aerodynamic drag force measurement

3. RESULTS AND DISCUSSION

Main results of the research are pressure coefficients and aerodynamic drags which evaluated in terms of reduction in the application of blowing active control. Figure 4 presents contour pathlines coloured by static pressure for models without active flow control for respective front slant angles.

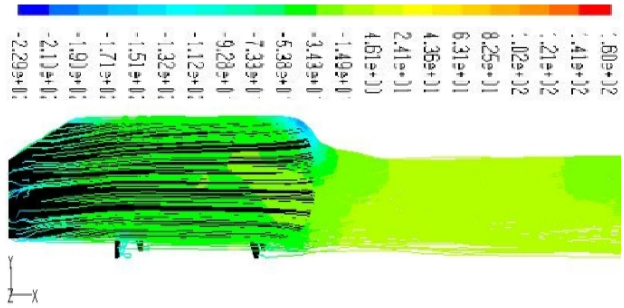

a. Vehicle model with θ=25°

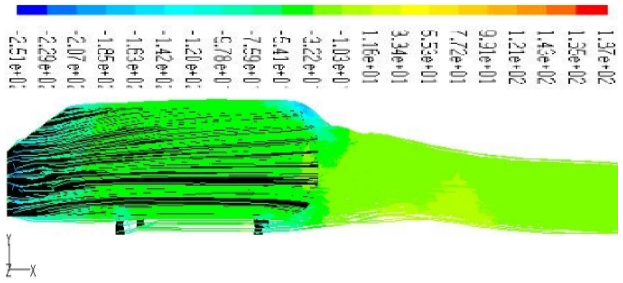

b. Vehicle model with θ=30°

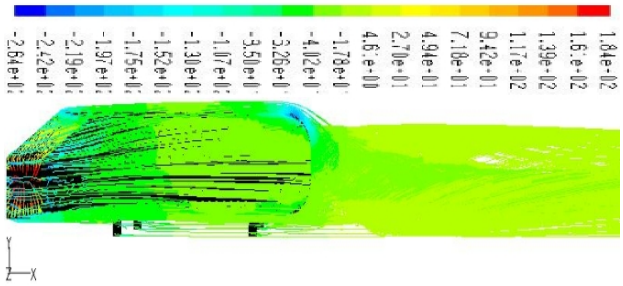

c. Vehicle model with θ=35°

Figure 4. Pathlines colored by static pressure without active flow control

The relationships of flow characteristics and vehicle's geometric parameters are presented in consecutive figures and tables. The first to be discussed is the expression of the distribution of pressure coefficient C_p in the relation to the so-called y/h ratio which is the ratio of the height of the grid to the height of vehicle model. The second will be the patterns of pressure coefficient distribution on the rear part of vehicle models in regards with z/w parameter, the ratio of width of grid to the width of vehicle models. The first one is shown in figure 6 for vehicle models with slant angle variations (θ) of 25°, 30°and 35°and given upstream velocity of 16.7 m/s.

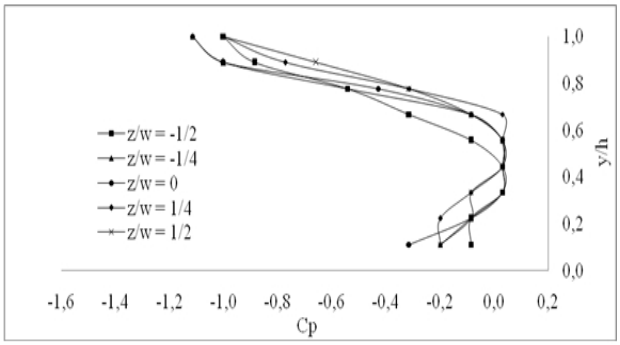

a. Vehicle model with θ=25°

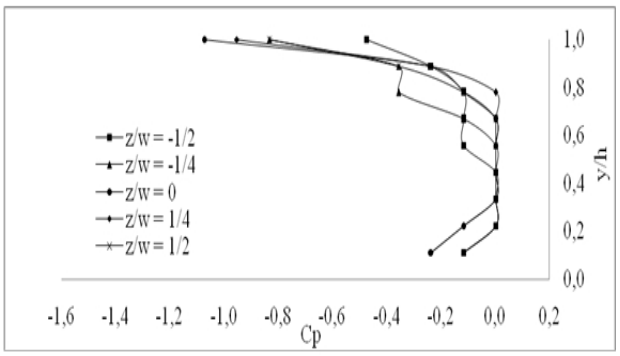

b. Vehicle model with θ=30°

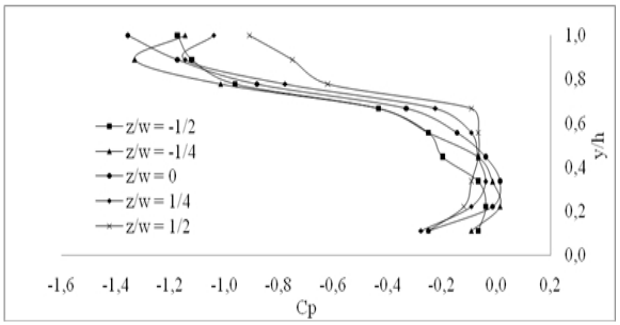

c. Vehicle model with θ=35°

Figure 6. The distribution of pressure coefficients without an active flow control

The minimum values of pressure coefficients on respective test model are presented in table 2 where, as shown in the table 2, the minimum value of pressure coefficients occurs at y/h=1, specifically on the edge of upper side of rear part of respective vehicle models. The highest pressure coefficient is recorded on the vehicle model with a 30° front slant angle as compared to the coefficients on models with 25°and 35°frontal slant angles. It is expected that a flow separation is likely to occur on the rear part of vehicle models, where the separation could induce back flow and therefore can reduce the pressure coefficient. This evidence is in agreement with the opinion of Anderson et al. [29].

Table 2, The minimum value of pressure coefficients without an active flow control

Vehicle model	Pressure coefficient, C_p	y/h	z/w
$\theta=25^0$	-1.1148	1	-1/4 and 0
$\theta=30^0$	-1.0716	1	0
$\theta=35^0$	-1,3556	1	0

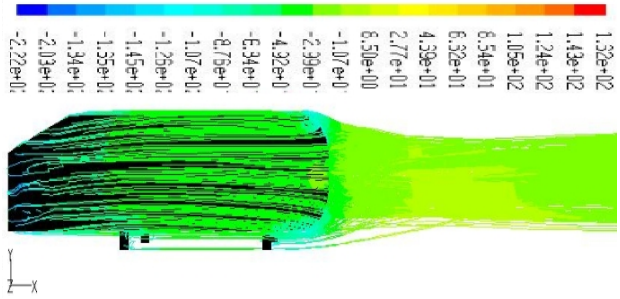

a. Vehicle model with θ = 25°

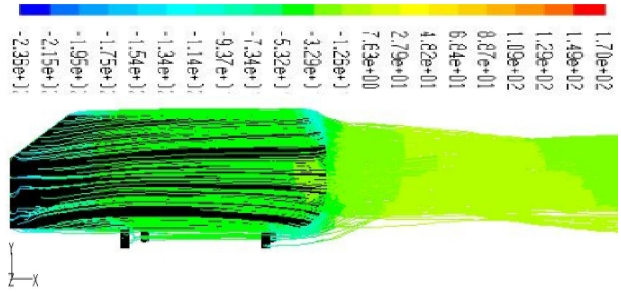

b. Vehicle model with θ = 30°

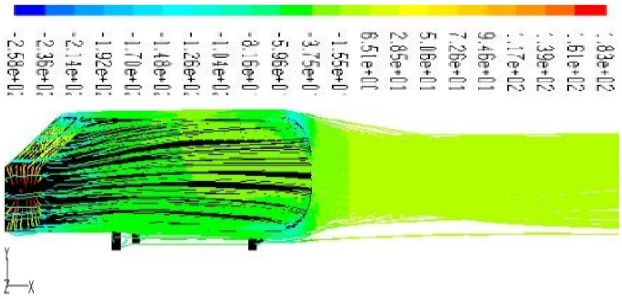

c. Vehicle model with θ = 35°

Figure 7. Pathlines colored by static pressure with blowing flow control

The presence of active control in the form of blowing was then evaluated based on the same parameter. Figure 7 presents contour pathlines colored by static pressure for models with the application of blowing active flow control for respective front slant angles. Figure 8 presents the distributions of pressure coefficients for given 16.7 m/s upstream velocity U_o as well as 0.5 m/s blowing velocity U_{bl}; all were applied on vehicle models with frontal slant angles of 25°, 30° and 35° respectively. The figures show that with the application of blowing flow control, the pressure coefficient tends to increase. From around y/h=0.6 to y/h=1, pressure coefficients start to change in a positive direction. This finding shows that on the upper side of the rear part of respective model, pressure coefficient increases. By the application of blowing flow control, the lower pressure stream, and considering the shape factor and friction of air with model's wall can be reduced therefore the flow separation the rear part of the test model can be reduced as well. Table 3 summarizes the minimum values of the pressure coefficient distribution on a 0.5 m/s given blowing velocity U_{bl} and a 16.7 m/s upstream velocity U_o. The table also shows that the smallest pressure coefficient distribution was on the model with a 30° front slant angle when compared to the test model with 25° and 35° slant angles.

Table 3. Minimum values of pressure coefficient with blowing flow control

Vehicle model	Pressure coefficient, C_p	y/h	z/w
$\theta=25^0$	-0.9622	1	1/4
$\theta=30^0$	-1.0285	1	-1/4
$\theta=35^0$	-0.8279	1	-1/4

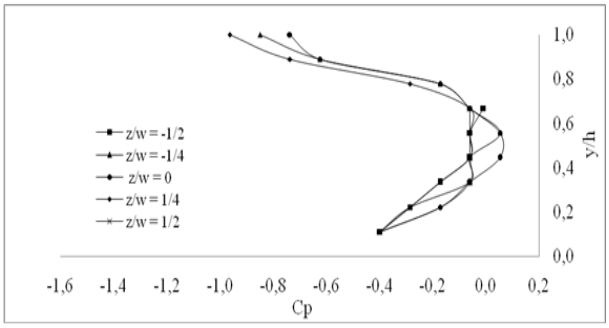

a. Vehicle model with θ = 25°

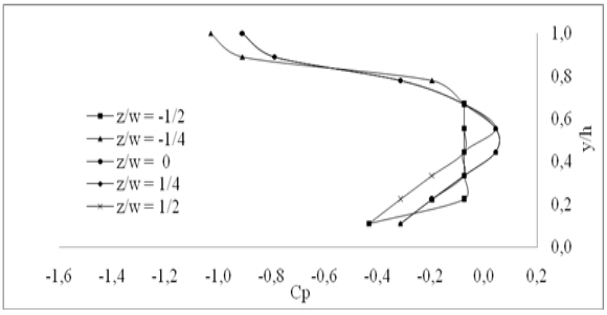

b. Vehicle model with θ = 30°

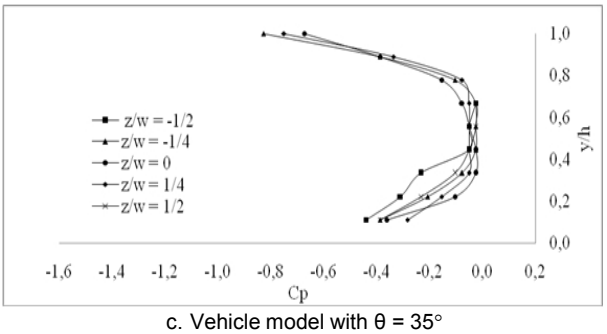

c. Vehicle model with θ = 35°

Figure 8. Pressure coefficient distribution with blowing flow control

The effect of additional active control by blowing with U_{bl}=0.5 m/s blowing speed in the reduction of the flow separation at the rear of each vehicle model is shown in table 4. The reduced flow separation gives an effect in the increase of the pressure coefficients on all vehicle models [30]. The largest value of increasing of pressure coefficient with the addition of blowing active control is on the model with 35° front slant angle gaining a number of percentages of 38.93%.

Table 4. Increasing pressure coefficient with blowing flow control

Vehicle model	Pressure coefficient, C_p		Increasing C_p, (%)
	Without active flow control	With blowing	
$\theta=25^0$	-1.1148	-0.9622	13.69
$\theta=30^0$	-1.0716	-1.0285	4.02
$\theta=35^0$	-1,3556	-0.8279	38.93

3.1 The computational method

Table 5 presented the aerodynamic drag coefficients for computational approach on the vehicle models with frontal slant angle of θ=25°, θ=30° and θ=35° both for normal treatment (without flow control) and with the addition blowing flow control with blowing speed U_{bl} of 0.5 m/s and upstream velocity U_o of 16.7 m/s.

Table 5. Aerodynamic drag coefficient and aerodynamic drag reduction by computational method

Vehicle model	Aerodynamic drag coefficient, C_d		Aerodynamic drag reduction, %
	without active flow control	with blowing	
$\theta=25^0$	1.7752	1.5639	11.90
$\theta=30^0$	1.6709	1.5699	6,04
$\theta=35^0$	1.7556	1.4953	14.81

Table 5 gives information that, in vehicle model without active control, the smallest aerodynamic drag coefficient is obtained in model with a 30° slant angle with the value of 1.6709 while on the models with 25°and 35° front slant angles, aerodynamic drag coefficients were 1.7752 and 1.7556 respectively. It is shown that the aerodynamic drag coefficients on each model were decreasing as the effect of the additional blowing active control while the smallest drag coefficient occurred in the model with θ=35°where the value of 1.4953. For models with θ=25° and θ=30°, the aerodynamic drag coefficients were 1.5639and 1.5699 respectively.

From the table 5 also, the largest reduction of aerodynamic drag as the effect of blowing flow control occurs on vehicle model with θ of 35° on a given 0.5 m/s blowing velocity U_{bl} and 16.7 m/s upstream velocity U_o with the reduction percentage was 14.81% . For the vehicle models with slant angles of 25°and 30°, the reduction were 11.90% and 6.04% respectively, as shown in table 5. The aerodynamic drag value on vehicle model with front slant angle 35° is capable to increase pressure coefficient on rear part of vehicle model for up to 38.93% as the effect of blowing flow control. The increasing of pressure coefficient on rear parts of vehicle models can decrease the aerodynamic drag. Results obtained from the research have confirmed the results of other researchers [16, 18, 23, 26, 27] where the application of active control by blowing can reduce aerodynamic drag on vehicle models.

3.2 The experimental method

Table 6 presents the aerodynamic drag coefficients obtained from experimental method on three vehicle models, which have similar geometric parameters to the model used for computational method.

Table 6. Aerodynamic drag coefficient and aerodynamic drag reduction by experimental method

Vehicle model	Aerodynamic drag coefficient, C_d		Aerodynamic drag reduction, %
	without active flow control	with blowing	
$\theta=25^0$	1.6237	1.4480	10.82
$\theta=30^0$	1.5173	1.4313	5.67
$\theta=35^0$	1.5655	1.3747	12.54

Table 6 gives the information that for models without flow control, the smallest aerodynamic drag coefficients occurs in the 30° front slant angle vehicle modelwith 1.5173 value as for models with θ=25°and θ=35°, the aerodynamic drag coefficients were 1.6237 and 1.5655 respectively. Additional blowing flow control for all models gives reduction of aerodynamic drag coefficients while the smallest aerodynamic drag coefficients occurred in the model with a 35°front slant angle with the value of 1.3747% and 1.4480% as well as 1.4313% for vehicle models with θ=25° and θ=30°.

From the table 6 also, it is obvious that the smallest reduction of aerodynamic drag by active control with blowing speed U_{bl} of 0.5 m/s and upstream velocity U_o of 16.7 m/s occurred on the model with θ=35° giving the reduction of 12.54% while on models with θ=25° dan θ=30° the reductions were 10.82% and 5.67% respectively.

The comparison of aerodynamic drag coefficients for vehicle models with θ=25°, θ=30°and θ=35° front slant angles obtained from both computational method as well as experimental method are shown on tables 7, 8 and 9 respectively.

Table 7 contains the comparison of aerodynamic drag coefficient for vehicle model with slant angle θ=25° from computational and experimental methods. It is shown that the aerodynamic drags coefficients from the two methods on models without flow control differ in about 8.53%, as for models with a 0.5 m/s blowing flow control, the two methods result a 7.41% difference in the value of aerodynamic drag coefficient. The table 7 also informs that there is a 1.08% slight difference in the reduction of aerodynamic drag coefficient for the two methods.

Table 7. Aerodynamic drag coefficient (C_d) for vehicle model with $\theta=25^0$

Description	Aerodynamic drag coefficient, (C_d)		Aerodynamic drag coefficient (C_d) reduction (%)
	without active flow control	with blowing	
Computational	1.7752	1.5639	11.90
Experimental	1.6237	1.4480	10.82
Difference	8.53%	7.41%	1.08

Table 8 shows the comparison of aerodynamic drag coefficients from both computational and experimental approaches for vehicle model with slant angle of θ=30°.The coefficients of aerodynamic drag of the two methods for models without flow control differ on 9.19% differences. For vehicle models with blowing flow control at blowing speed of 0.5 m/s, the two methods give 8.83% difference in aerodynamic drag coefficient values. The table 8 also shows that the reduction of aerodynamic drag coefficients between computational and experimental methods differ on only 0.37%.

Table 8. Aerodynamic drag coefficient (C_d) for vehicle model with θ=30^0

Description	Aerodynamic drag coefficient, (C_d)		Aerodynamic drag coefficient (C_d) reduction (%)
	without active flow control	with blowing	
Computational	1.6709	1.5699	6.04
Experimental	1.5173	1.4313	5.67
Difference	9.19%	8.83%	0.37

Table 9. Aerodynamic drag coefficient (Cd) for vehicle model with θ=350

Description	Aerodynamic drag coefficient, (C_d)		Aerodynamic drag coefficient (C_d) reduction (%)
	without active flow control	with blowing	
Computational	1.7556	1.4953	14.81
Experiment	1.5655	1.3706	12.54
Difference	10.82%	8.34%	2.27

Aerodynamic drag coefficients obtained from computational and experimental methods for θ=35° model are listed in table 9. For models without flow control, the aerodynamic drag coefficients of the two methods have 10.82% differences. On vehicle models with active blowing flow control at blowing speed of 0.5 m/s, the two methods give 8.34% difference in aerodynamic drag coefficient values. The table 9 also shows that the reductions of aerodynamic drag coefficients of the two methods differ about 2.27%.

4. CONCLUSION

Based on the results of pressure coefficients and drag reduction on reversed Ahmed vehicle models with front slant angles (θ) of 25°, 30° and 35° as well as the application of blowing flow control, some conclusion can be drawn. It is obvious that the active flow control by blowing and variations on front geometry provide significant impact to the increasing of pressure coefficients and reduction of aerodynamic drag. The most significant increase on pressure coefficients occurs on vehicle model with the 35° front slant angle, gaining 38.93% value, where pressure coefficients with and without blowing flow control reach -0.8279 and -1.3556, respectively. In terms of aerodynamic drag reduction, vehicle model with the 35° front slant angle also gains the value of 14.81 and 12.54 for computational and experimental methods, while the reductions of aerodynamic drag coefficients of the two approaches have 2.27% difference.

ACKNOWLEDGEMENTS

The research was funded by the Ministry of Research, Technology and Higher Education through University Excellence Scheme F.Y 2018, with Research Contract No. : 1579/UN4.21/PL.00.00/2018, dated March 21th 2018.

REFERENCES

[1] Agarwal, R.K."Sustainable ground transportation – review of technologies, challenges and opportunities", International Journal of Energy and Environment, Vol. 4, No.6, pp.1061-10782013, 2013.

[2] Ahmed, S., Ramm, G., Faltin, G."Some Salient Features Of The Time-Averaged Ground Vehicle Wake", SAE Technical Paper 840300, 1984.

[3] Sims-Williams, D., Dominy, R. "Experimental Investigation into Unsteadiness and Instability in Passenger Car Aerodynamics", SAE Technical Paper 980391, 1998.

[4] Bayraktar, I., Landman, D., Baysal, O. "Experimental and Computational Investigation of Ahmed Body for Ground Vehicle Aerodynamics", SAE Technical Paper 2001-01-2742, 2001.

[5] Joseph, P., Amandolese, X., Edouard, C. Aider, J. "Flow control using MEMS pulsed micro-jets on the Ahmed body", Experiment in Fluids, Vol. 54, No. 1, 1442, 2013.

[6] Lienhart, H., Becker, S. "Flow and Turbulence Structure in the Wake of a Simplified Car Model", SAE Technical Paper 2003-01-0656, 2003,

[7] Han, T. "Computational analysis of three-dimensional turbulent flow around a bluff body in ground proximity", AIAA Journal, Vol. 27, No.9, 1989, pp. 1213-1219.

[8] Basara, B., Przulj, V., Tibaut, P. "On the Calculation of External Aerodynamics: Industrial Benchmarks", SAE Technical Paper 2001-01-0701, 2001.

[9] Basara, B. "Numerical simulation of turbulent wakes around a vehicle", in: *ASME Fluid Engineering Division Summer Meeting FEDSM99-7324*. San Francisco, USA, 1999.

[10] Basara, B., Alajbegovic, A. "Steady state calculations of turbulent flow around Morel body". in: *7th International Symposium of Flow Modelling and Turbulence Measurements*, Taiwan, 1998, pp. 1–8

[11] Gilliéron, P.,Chometon, F. "Modeling of stationary three-dimensional separated air flows around an Ahmed reference model", in : *ESAIM, Proceeding of Third International Workshop on Vortex Flows and Related Numerical Methods*, 7, 1999, pp. 173–182.

[12] Kapadia, S., Roy, S., Vallero, M., Wurtzler, K., Forsythe J. "Detached-Eddy Simulation over a Reference Ahmed Car Model", in: Friedrich, R., Geurts, B.J., Métais, O. (eds*) Direct and Large-Eddy Simulation V*. ERCOFTAC Series, 9. Springer, Dordrecht, 2004, pp 481-488.

[13] Conan, B., Anthoine, J., Planquart, P. "Experimental aerodynamic study of a car-type bluff body", Experiments in Fluids, Vol. 50, No. 5, pp.1273-1284, 2010.

[14] Krogstad, P.A., Kourakine, A. "Some effects of localized injection on the turbulence structure in a boundary layer", Physics of Fluids, Vol. 12, No.11, pp. 2990-2999, 2000.

[15] Park, J., Choi, H. "Effects of uniform blowing through blowing or suction from a spanwise slot on a turbulent boundary layer flow", Physics of Fluids, Vol. 11, No. 10, pp. 3095–3105, 1999.

[16] Krentel D., Muminovic R., Brunn A., Nitsche W., King R. "Application of Active Flow Control on Generic 3D Car Models". in: King R. (eds) *Active Flow Control II. Notes on Numerical Fluid Mechanics and Multidisciplinary Design*, 108. Springer, Berlin-Heidelberg, Germany, 2010, pp. 223-239.

[17] Heinemann, T., Springer, M., Lienhart, H. "Active flow control on a 1:4 car model", Experiments in Fluids, Vol. 55, No. 5, 1738, 2014.

[18] Mestiri, R., Ahmed-Bensoltane, A., Keirsbulck, L., Aloui, F.,Labraga, L. "Active Flow Control at the Rear End of a Generic Car Model Using Steady Blowing", Journal of Applied Fluid Mechanics, Vol. 7, No. 4, pp. 565-571, 2014.

[19] Tounsi, N., Mestiri, R., Keirsbulck, L., Oualli, H., Hanchi, S., Aloui, F."Experimental Study of Flow Control on Bluff Body using Piezoelectric Actuators" , Journal of Applied Fluid Mechanics , Vol. 9, No. 2, pp. 827-838, 2016.

[20] Tian, J., Zhang, Y., Zhu, H., Xiao, H."Aerodynamic drag reduction and flow control of Ahmed body with flaps", Advances in Mechanical Engineering, Vol. 9, No.7, pp. 1–17, 2017.

[21] Shadmani, S., Mousavi-Nainiyan, S.M., Ghasemiasl, R.,Mirzaei, M., Pouryoussefi, S.G. "Experimental Study of Flow Control Over an Ahmed Body Using Plasma Actuator", Mechanics and Mechanical Engineering, Vol. 22, No. 1, pp. 239–251, 2018.

[22] Prakash, B., Bergada, J.M., Mellibovsky, F. "Three Dimensional Analysis of Ahmed Body Aerodynamic Performance Enhancement using Steady Suction and Blowing Flow Control Techniques", in : *Tenth International Conference on Computational Fluid Dynamics (ICCFD10)*, 2018. Barcelona, Spain.

[23] Harinaldi, Budiarso, Tarakka, R., Simanungkalit, S.P. "Effect of Active Control by Blowing to Aerodynamic Drag of Bluff Body Van Model", International Journal of Fluid Mechanics Research, Vol. 40, No.4, pp. 312-323, 2013.

[24] Julian, J., Karim, R.F., Budiarso, Harinaldi, "Review: Flow Control on a Squareback Model" International Review of Aerospace Engineering (IREASE), Vol. 10, No. 4, pp. 230-239, 2017.

[25] Harinaldi, Budiarso, Warjito, Kosasih, E.A., Tarakka, R., Simanungkalit, S.P. "Active technique by suction to control the flowstructure over a van model", Journal of Engineering and Applied Science, Vol. 7, No. 2, pp.215-222, 2012.

[26] Harinaldi, Budiarso, Tarakka, R., Simanungkalit, S.P. "Computational Analysis of Active Flow Control to Reduce Aerodynamics Drag on a Van Model", International Journal of Mechanical & Mechatronics Engineering IJMME-IJENS, Vol. 11, No. 3, pp. 24-30, 2011

[27] Tarakka, R., Jalaluddin, Mire, B., Umar, M.N. "Effect of Turbulence Model In Computational Analysis of Active Flow Control on Aerodynamic Drag of Bluff Body Van Model", International Journal of Applied Engineering Research, Vol. 10, No. 1, pp. 207-219, 2015.

[28] Tarakka, R., Salam, N., Jalaluddin, Ihsan, M. "Active Flow Control by Suction on Vehicle Models with Variations on Front Geometry', International Review of Mechanical Engineering, Vol. 12, No. 2, 2018, pp. 128-134.

[29] Anderson, J.D. "Fundamental of Aerodynamics" 3rd ed., McGraw-Hill, Singapore, 2001.

[30] Sphon, A., Gilliéron, P. "Flow separations generated by simplified geometry of an automotive vehicle", in: *IUTAM Symposium: Unsteady separated flows*, 2002, Toulouse, France.

NOMENCLATURE

Cd	drag coefficient
Cp	pressure coefficient
Fd	pressure drag force [N]
h	height of test model [m]
l	length of test model [m]
ρ	density [kg/m^3]
θ	front slant angle [^{o}]
Re	Reynolds number
S	cross section area [m^2]
τ_w	wall shear stress [N/m^2]
U_{bl}	blowing velocity [m/s]
U_o	upstream velocity [m/s]
μ	viscosity [N.s/m^2]
w	width of test model [m]

2. Informasi artikel telah direview oleh Reviewer FME Transctions (1 Desember 2018)

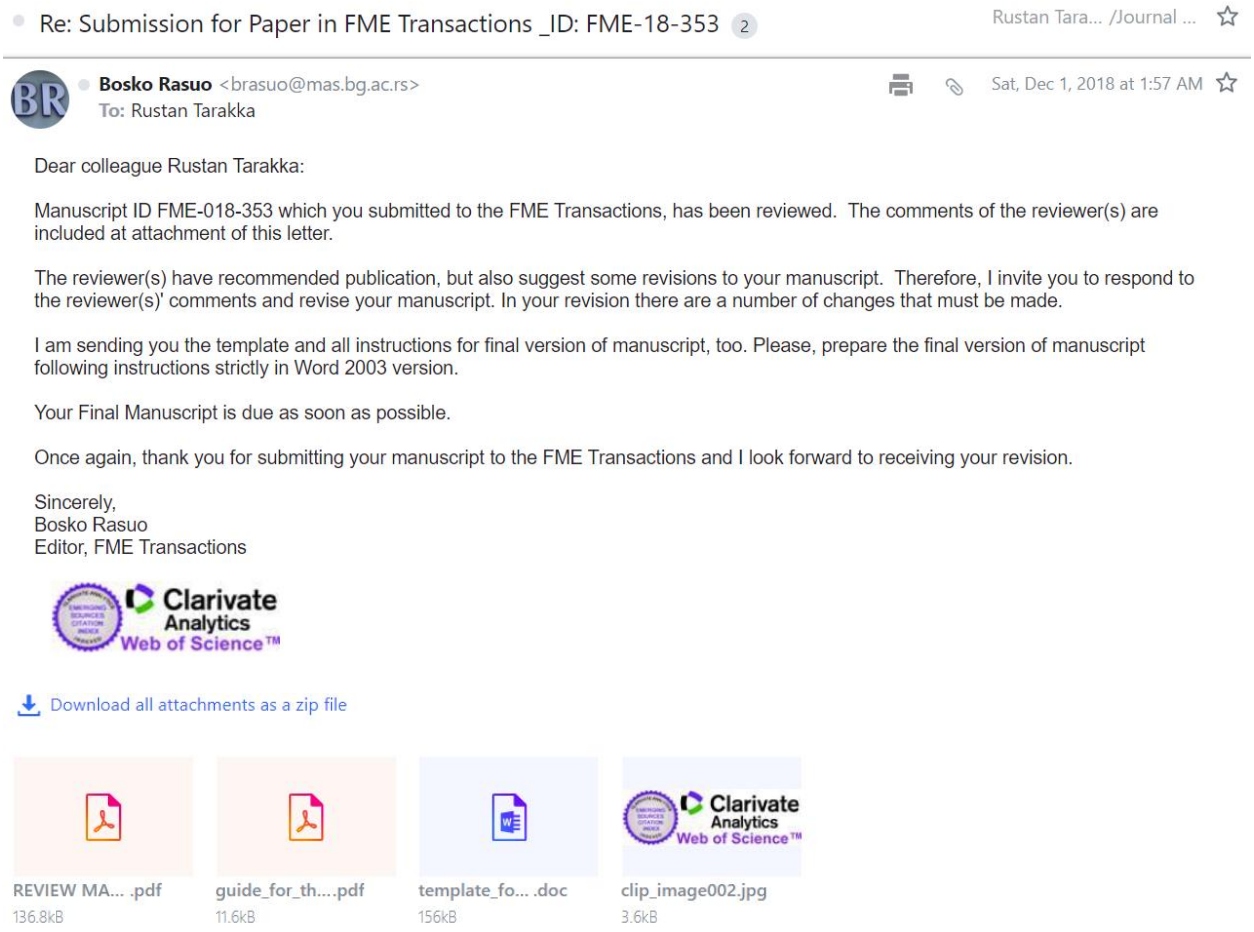

Re: Submission for Paper in FME Transactions _ID: FME-18-353 2

Rustan Tara... /Journal ...

Bosko Rasuo <brasuo@mas.bg.ac.rs>
To: Rustan Tarakka

Sat, Dec 1, 2018 at 1:57 AM

Dear colleague Rustan Tarakka:

Manuscript ID FME-018-353 which you submitted to the FME Transactions, has been reviewed. The comments of the reviewer(s) are included at attachment of this letter.

The reviewer(s) have recommended publication, but also suggest some revisions to your manuscript. Therefore, I invite you to respond to the reviewer(s)' comments and revise your manuscript. In your revision there are a number of changes that must be made.

I am sending you the template and all instructions for final version of manuscript, too. Please, prepare the final version of manuscript following instructions strictly in Word 2003 version.

Your Final Manuscript is due as soon as possible.

Once again, thank you for submitting your manuscript to the FME Transactions and I look forward to receiving your revision.

Sincerely,
Bosko Rasuo
Editor, FME Transactions

Clarivate Analytics Web of Science™

Download all attachments as a zip file

REVIEW MA... .pdf 136.8kB

guide_for_th....pdf 11.6kB

template_fo... .doc 156kB

clip_image002.jpg 3.6kB

FME TRANSACTIONS

Journal of

Faculty of Mechanical Engineering,

University of Belgrade

Kraljice Marije 16, 11120 Belgrade 35, Serbia

Date Submitted by the Author: .....

Manuscript ID: FME-018-353

Total Time in Review: .....

MANUSCRIPT REVIEW FORM

Author(s): Rustan Tarakka et al.			
Paper title: Effect of blowing flow control and front geometry towards the reduction of aerodynamic drag on vehicle models			
1.	Does the paper correspond to the topics covered by the Journal?	**Yes** ✓	**No**
2.	Do you recommend the paper for publication in the Journal?	**Yes** ✓	**No**
3.	Recommendation	**Without change:** **After minor revision:** ✓ **After major revision:** **Reject:**	
4.	Would you like to review a revision of this manuscript?	**Yes**	**No**

Confidential data

Date: .30.11.2018. Reviewer:

Please sign this copy:

COMMENTS OF REFEREE:

Results obtained by the CFD analyses differ by some 8 – 10% from those obtained by the experiment, which is at the edge of tolerance even for preliminary analyses. On the other hand, relative improvements obtained by both methods are quite similar, which enables drawing of practical conclusions. Paper could be published, but with the following changes included:

1) It should be written what (if any) wind tunnel corrections have been applied on the "raw" experimental results. Uncorrected results could be one of the sources of the obtained differences between the CFD and experiment.

2) It is mandatory to at least mention what governing equations and turbulence model have been used in the CFD analyses.

3) Considering the mesh, it should be shown in one or two pictures (for example, the complete control volume domain and in the vicinity of the Ahmed model), state the number of mesh elements, present if calculation has been made oh half model with symmetry plane or full model, etc.

4) The text in Fig. 3, describing the experimental facility, is too small and hardly readable. Text must be enlarged so that it can normally be read on a hard-copy version of the paper.

5) Graphics in Figs. 4 and is blurred, and those pictures must be replaced by higher quality graphics.

6) In table 1, the boundary conditions should be stated as:

Outlet: Pressure outlet
Inlet: Velocity inlet

(the original text sais: Pressure outlet: Pressure outlet Velocity inlet: Velocity inlet)

7) It is recommendable for the authors to try to find some appropriate references from the FME Transactions journal, in order to underline the connections of the manuscript with the aims and scope of the Journal, like:

Ocokoljić, G., Damljanović, D., Vuković, Đ., Rašuo, B.: Contemporary Frame of Measurement and Assessment of Wind-Tunnel Flow Quality in a Low-Speed Facility, FME Transactions, Vol. 46, No. 4, pp. 429-442, 2018, doi:10.5937/fmet1804429O.

Ocokoljić, G., Damljanović, D., Rašuo, B., Isaković, J.: Testing of a Standard Model in the VTI's Large-subsonic Wind-tunnel Facility to Establish Users' Confidence, FME Transactions, Vol. 42, No. 3, pp. 212-218, 2014, doi:10.5937/fmet1403212O.

Aims and Scope:

The journal FME Transactions publishes original papers (reviewing and contributed papers, and short communications) from all fields of Mechanical Engineering, which is, as a branch of Engineering, considered in the journal in its broadest possible sense. Thus, the articles are welcome from: Applied Mechanics, Fluids Engineering, Thermodynamics, Heat and Mass Transfer, Robotics, Material Science, Tribology, Combustion, Mechanical Design and Machine Dynamics, Productional, Industrial, Agricultural, Aerospace, Processing, Railway, Biomedical and Control Engineering, Mechanization, Hydro- and Thermo-power Systems, Internal Combustion Engines and Vehicle Dynamics, Energy Resources Technology, Military Technology, Naval Architecture, and Applied and Industrial Mathematics.

Theoretical, experimental and computational analyses of various problems of Mechanical Engineering are equally welcome and acceptable for publication. In addition, there will be published book reviews, announcements of symposia, and in special issues, proceedings of selected papers from symposia organized by the Faculty of Mechanical Engineering in Belgrade.

Reviewing papers will be published by invitation only. One volume consists of four numbers.

Instructions for Authors:

A FME Transaction manuscript should by written clearly and concisely in correct English, with assumptions clearly identified, with precise logic, with relevance to practice described, and with actual accomplishments of the work plainly stated and honestly appraised. Normally, the length of a reviewing paper is up to 12 pages, the length of a contributed paper is up to 8 pages, while the length of a short communication should not exceed 4 pages. All papers are subject to a reviewing process. During the process the names of referees will be kept confidential to authors, and also the names of authors will remain anonymous to referees. As a rule the reviewing process should be accomplished in 2-3 months. Final acceptance of a paper for publication in the Journal is based on the decision of the Editorial Board.

Template for Manuscript:

http:/www.mas.bg.ac.rs/transactions

Submission of Papers:

Papers intended for publication in FME Transactions should be submitted to the Editor, in the electronic or the hard-copy form, to the following address:

fme-transactions@mas.bg.ac.rs

or:

Prof. Bosko Rasuo, Editor
Faculty of Mechanical Engineering
Kraljice Marije 16,
11120 Belgrade 35
Serbia

Three copies of the manuscript and the compact disc (CD) should be accompanied by a letter, signed by all authors, declaring that the material of the paper has not been previously published in full or in a substantial part in another journal, book or proceedings, as well as that it has not been submitted for publication elsewhere.

First A. Author
(Helvetica 10 pt, bold)
Affiliation-Professor
Institution or Company-
University of Belgrade
Faculty of Mechanical Engineering
(Helvetica 7,5 pt)

Second B. Author
(Helvetica 10 pt, bold)
Teaching Assistant
University of Novi Sad
Faculty of Technical Sciences
(Helvetica 7,5 pt)

Third C. Author
(Helvetica 10 pt, bold)
Assistant Professor
University of Nis
Faculty of Mechanical Engineering
(Helvetica 7,5 pt)

Title (Helvetica 16 pt, bold)

Type the abstract of not more than 150 words outlining description of the problem, method used and conclusions. The abstract is an essential part of the paper. Use short, direct, and complete sentences. It should be as brief as possible and concise. It should be complete, self-explanatory, and does not require reference to the paper itself. The abstract should be informative, giving the scope and emphasizing the main conclusions, results, or significance of the work described. Do not use first person; do not include mathematical expressions; do not refer to the reference, and try to avoid acronyms. Use this document as a template for MS Word, version 97 or later. Otherwise, use this document as an instruction set (Times New Roman 10 pt, Italic).

Keywords (Times New Roman 10 pt, Bold): *5-8 keywords, left justified (Times New Roman 10 pt, Italic).*

1. INTRODUCTION (ALL CAPS - HELVETICA 9 PT, BOLD) - ALIGN LEFT

These are instructions for authors typesetting for the Journal FME TRANSACTIONS. This document has been prepared using the required format. The paper must be written in correct English (English or American spelling). If the quality of the language is too poor, this can prevent your paper from being included in the Proceedings. For the good appearance of the Proceedings it is of intrinsic importance that all full texts are of the same shape. The paper is to be written in two-column format on the paper size A4 and be right and left justified, using single spacing (Times New Roman 10) The width of all margins is to be 20 mm. The width of each column is to be 80 mm, and the gap between columns should be 10 mm (Format>Columns).

The paragraph indentation is to be 5 mm (Format>Paragraph>Indents and Spacing>Special: First line by 5 mm).

Leave one clear line before and after a main or secondary heading.

We recommend to start with an Introduction where you formulate your problem or task respectively, present the state-of-the-art and establish the position of your work in the international scene.

2. MAIN HEADING (CAPITAL LETTERS, ALIGN LEFT - HELVETICA 9 PT, BOLD)

Please use this document as a template to prepare your manuscript.

In left bottom corner put the full mailing and email addresses of the corresponding author and his affiliation, as presented below.

Received: January 2008, Accepted: March 2008
Correspondence to: Dr John Smith
Faculty of Mechanical Engineering,
Kraljice Marije 16, 11120 Belgrade 35, Serbia
E-mail: jsmith@mas.bg.ac.rs

2.1 Secondary heading (Helvetica 9 pt, bold) – Align left

Avoid leaving a heading at the bottom of a column, with the subsequent text starting at the top of the next page/column.

Do not use further subdivision, for instance 2.1.1. is not allowed.

Use Word program Equations editor to type all formulas (size 10). For subscripts and superscripts use letter size 8. Denotation typewritten in the text should be set in italic, size 10.

Mathematical formulas should be centred and have to be numbered consecutively from 1 in parentheses on the far right margin of the column, as formula (1):

$$\frac{\mathrm{d}\delta_2}{\mathrm{d}x} + (2\delta_2 + \delta_1)\,\frac{\bar{u}'_{\mathrm{e}}}{\bar{u}_{\mathrm{e}}} = \frac{\tau_{\mathrm{w}}}{\rho \bar{u}_{\mathrm{e}}^2} + \frac{\nu}{\bar{u}_{\mathrm{e}}^2}\,\delta\,\left(\frac{\partial^2 \bar{u}}{\partial y^2}\right)_{\mathrm{e}}. \qquad (1)$$

Equations are separated by 6 points from the rest of the text, for example, (Format>Paragraph>Indents and Spacing>Spacing>Before 6 pt, After 6 pt).

All numbers and brackets in the text and formulas are to be vertical.

All variables: *a*, *b*, ... , *x*, *y*, *z*, should be set in italic, while the mathematical operators and functions should be vertical, as for example:

$$\frac{\mathrm{d}y}{\mathrm{d}x},\ \sin x,\ \cos x,\ \log x,\ \max,\ \min,\ \lim_{x\to\infty} f(x)\ . \qquad (2)$$

Indexes should be set according to the pre-given rules, i.e. if index is a number or a letter it should be set vertically. However, if index presents a symbol of a variable it should be set in italic, as for instance:

$$Nu_x = \frac{\varphi D}{[\lambda_{\mathrm{f}}\,(T_{\mathrm{s}} - T_{\mathrm{amb}})]} = \frac{h_x D}{\lambda_{\mathrm{f}}}\,. \qquad (3)$$

Vectors are to be written with arrow head as presented below:

$$\vec{\omega} = \frac{1}{2}\,\mathrm{rot}\,\vec{v}\,,\ \mathrm{div}\,\vec{v} = 0\,, \tag{4}$$

or should be set in bold:

$$\boldsymbol{\omega} = \frac{1}{2}\,\mathrm{rot}\,\mathbf{v}\,,\ \mathrm{div}\,\mathbf{v} = 0\,. \tag{5}$$

Nondimensional numbers as e.g. Reynold's, should be set in italic:

$$Re, \ldots \tag{6}$$

Full point and comma have to be typewritten in the text and not in Word Equation Editor.

Refer to (1), not to Eq. (1), or equation (1), except at the beginning of a sentence. Be sure that the symbols in your equation have been defined before the equation appears or immediately following.

SI units are strongly encouraged. Do not use English units. Avoid combining different units. This often leads to confusion because equations do not balance dimensionally. If you must use mixed units, clearly state the units for each quantity in an equation.

Units should be typewritten vertically, as for example:

$$p = 10\,\mathrm{N/m^2} \quad \text{or} \quad p\ [\mathrm{N/m^2}]\,.$$

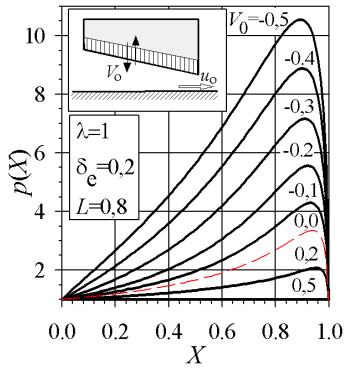

Figure 1. Title (Helvetica 8 pt, bold) – Align left

Restrict figures to single-column width unless this would make them illegible. If necessary for the purpose of clarity they can be spread over both columns. Coloured figures will be reproduced in colour only in electronic version of the Journal, while they will not be reproduced in colour in printed version, so it is not recommended to use coloured figures and photographs. If possible, do not assemble figures at the back of your article, but place them as close as possible to where they are mentioned in the main text.

Figures, numbered consecutively with captions, should be incorporated into the main body of the text. Do not put figures in frames.

Do not insert text along the figure by using Insert + Tex Box. Do not put captions in text boxes linked to the figures. Do not put borders around the outside of your figures.

Figures should be centred (Format Object + Layout + In line with text).

No part of a figure should go beyond the typing area. Captions should appear below graphical objects.

Figures are to be inserted in their proper place throughout the paper and not to be grouped together. Please use only drawings and photographs of excellent quality. It is especially important that all numbers and characters appearing in your figures are of good quality and well-readable size (≈8-10 pt), i.e. approximately of the same size as your text. Figure axis labels are often a source of confusion. Axes labels must be clearly denoted. Figure labels should be legible, approximately 8 to 10 point type.

Captions should appear below graphical objects. Captions are the part of the text and not of the figures. Number and title of the figure are separated from figure and main text by 6 pt (Format>Paragraph>Indents and Spacing>Spacing>Before 6 pt, After 6 pt), as shown in these instructions.

All tables should be incorporated into the main body of the text and must be centred in the column and numbered consecutively (in Arabic numbers).

Place tables as close as possible to where they are mentioned in the main text. Large tables may span both columns.

Table headings should be placed above the table, as shown in this template. The width of all lines in tables including all borders should be 1/2 pt. Text and numbers in tables should be typewritten in Times New Roman, 9 pt.

Table 1. Heading (Helvetica 8 bold) – Align left

Element	Chemical composition (%)			
	SiO_2	Al_2O_3	Fe_2O_3	CaO
Cordierite (C)	45.52	28.10	1.23	3.70
Talc (T)	62.20	3.11	1.25	1.07

It is recommended that footnotes be avoided. Instead, try to integrate the footnote information into the text.

Define abbreviations and acronyms the first time they are used in the text, even they have already been defined in the abstract. Do not use abbreviations in the title unless they are unavoidable (for example “ASME”).

References to relevant literature are to be given in usual format, please consult the sample references at the end of theses instructions. References are to be listed in the order of their appearance in the text and numbered. Citation is by the number only which is to be put in square brackets, i.e. [1], [2], ... etc.

3. CONCLUSION (HELVETICA 9 BOLD) - ALIGN LEFT

A conclusion section is not required, but it is strongly recommended. Although a conclusion may review the main points of the paper, do not replicate the abstract as the conclusion. A conclusion might elaborate on the importance of the work or suggest applications and extensions.

APPENDIX (HELVETICA 9 BOLD, ALIGN LEFT)

Appendixes, if needed, appear before the acknowledgment. Do not include page numbers in the text.

ACKNOWLEDGMENT (HELVETICA 9 BOLD, ALIGN LEFT)

Use the singular heading even you have many acknowledgments. Also put in this section sponsor and financial support acknowledgments.

REFERENCES (HELVETICA 9 BOLD, ALIGN LEFT)

In the reference list, journal papers [1], books [2], multi-author books [3], theses [4] and conference Proceedings [5] should be cited as in the following examples:

[1] Beskok, A., Karniadakis, G.E. and Trimmer, W.: Rarefaction and compressibility effects in gas microflows, Trans. ASME - J. Fluids Eng, Vol. 118, No. 3, pp. 448-456, 1996.

[2] Gross, A. W.: *Gas film lubrication*, John Wiley and Sons, New York, 1992.

[3] Stachowiak, G.W.: Numerical Characterization of wear particle morphology, in: Hutchings, I.M. (Ed.): *New Directions in Tribology*, Mechanical Engineering Publications Ltd., Bury St Edmunds, pp. 371-389, 1997.

[4] Stokes, J.: *Production of Coated and Free-Standing Engineering Components using the HVOF (High Velocity Oxy-Fuel) Process*, PhD thesis, School of Mechanical and Manufacturing Engineering, Dublin City University, Dublin, 2003.

[5] Lancaster, J.K.: Severe metallic wear, in: *Proceedings of the Conference on Lubrication and Wear*, 01-03.10.1957, London, pp. 1-7 or Paper 72.

Please note that all references listed here must be directly cited in the body of the text. Please do not cite only your work or reports, but give proper reference to relevant related work of easy access, i.e. cite books and articles in journals and conference Proceedings, preferably in English.

If the reference has not been written in English, please translate it into English, and state the original language in brackets, e.g. (in Serbian).

Nomenclature should be put after references, but it is not required.

NOMENCLATURE (HELVETICA 9 PT, BOLD, ALIGN LEFT)

a_{f}	thermal diffusivity for fluid, (Times New Roman 10) $a_{\mathrm{f}} = \lambda_{\mathrm{f}}/(\rho c_p)$
h_x	local heat transfer coefficient

Greek symbols (Times New Roman 10 pt, bold, italic)

δ_{ij}	Kronecker delta
τ_{ij}	Reynolds or turbulent stress $\tau_{ij} = -\rho\overline{u_i u_j}$

Superscripts (Times New Roman 10 pt, bold, italic)

co	convective section
f	furnace section

Table 2. Heading – Large tables and figures may span both columns, and if it is not possible to incorporate them in the main text you can position them at the end of the paper (Helvetica 8 bold).

Term	Normal components of Reynolds stress		
	$\overline{u_1u_1}$	$\overline{u_2u_2}$	$\overline{u_3u_3}$
$-\mathcal{R}_{\tau,ij}^{II}/\rho$	$-0,4\overline{u_2u_2}\frac{\partial U_2}{\partial x_2} - 0,4\overline{u_3u_3}\frac{\partial U_3}{\partial x_3}$	$0,8\overline{u_2u_2}\frac{\partial U_2}{\partial x_2} - 0,4\overline{u_3u_3}\frac{\partial U_3}{\partial x_3}$	$-0,4\overline{u_2u_2}\frac{\partial U_2}{\partial x_2} + 0,8\overline{u_3u_3}\frac{\partial U_3}{\partial x_3}$
$-\mathcal{R}_{\tau,ij}^{\mathrm{w},II}/\rho$	$-0,12 f_{\mathrm{w}}\overline{u_2u_2}\frac{\partial U_2}{\partial x_2} +$ $+0,24 f_{\mathrm{w}}\overline{u_3u_3}\frac{\partial U_3}{\partial x_3}$	$-0,12 f_{\mathrm{w}}\overline{u_2u_2}\frac{\partial U_2}{\partial x_2} +$ $+0,24 f_{\mathrm{w}}\overline{u_3u_3}\frac{\partial U_3}{\partial x_3}$	$0,24 f_{\mathrm{w}}\overline{u_2u_2}\frac{\partial U_2}{\partial x_2} +$ $-0,48 f_{\mathrm{w}}\overline{u_3u_3}\frac{\partial U_3}{\partial x_3}$

3. Revisi artikel berdasarkan komentar Reviewer FME Transaction (7 Desember 2018)

Revision of Paper ID FME-018-353 2

Rustan Tara... /FME

Rustan Tarakka <rustan_tarakka@yahoo.com>
To: brasuo@mas.bg.ac.rs

Fri, Dec 7, 2018 at 10:21 AM

Dear Prof. Bosko Rasuo
Editor FME Transaction

Thank you very much for your prompt response regarding our paper submission, Paper ID: FME-018-353, titled : Effect of blowing flow control and front geometry towards the reduction of aerodynamic drag on vehicle models.

We have revised the paper according the recommendations from the referee with new text insertion in red color.

We are really hoping that the revision has met the referee's desire
and the paper is eligible to be published.

Thank you very much,

Dr. Rustan Tarakka
Dept. of Mechanical Engineering
Hasanuddin University

FME_Transa... .doc
1MB

Effect of blowing flow control and front geometry towards the reduction of aerodynamic drag on vehicle models

Rustan Tarakka
Assistant Professor
Hasanuddin University
Department of Mechanical Engineering
Indonesia

Nasaruddin Salam
Professor
Hasanuddin University
Department of Mechanical
Indonesia

Jalaluddin
Associate Professor
Hasanuddin University
Department of Mechanical Engineering
Indonesia

Muhammad Ihsan
Lecturer
Sekolah Tinggi Teknik Baramuli
Department of Civil Engineering
Indonesia

This paper presents analyses of the effect of blowing flow control and variations on front geometry towards the reduction of aerodynamic drag on vehicle models. Blowing flow control is an alternative measure in modifying the onset of flow separation in the boundary layer on the surface of the vehicle. The modification is expected to reduce the dominating influence of the separation area on the total drag. Conducted in computational and experimental approaches, the research investigated the effect of frontal slant angle variations (θ) of 25°, 30° and 35° towards the reduction of aerodynamic drag on vehicle models on the application of blowing flow control with upstream and blowing speed of 16.7 m/s and 0.5 m/s, respectively. Load cells were used in the experimental method to validate the reduction of aerodynamic drag obtained from computational method. It is indicated that the effects of blowing flow control and variations on front geometry are significant in the increasing on pressure coefficients and the reduction of aerodynamic drag on vehicle models. The largest increase on pressure coefficients of 38.93% is indicated on the vehicle model with θ=35°, while the largest reduction of aerodynamic drag occurred on the same model with the values of 14.81 and 12.54 for computational and experimental methods, respectively.

Keywords: *active flow control, aerodynamic drag reduction, blowing, front geometry, vehicle model.*

1. INTRODUCTION

As one of the most preferred types of general vehicles, family car in the form of multi purposed van (MPV) has both advantages and drawbacks. Of the drawbacks, one typical character is the demand of relatively larger capacity engine which means larger fuel consumption than its more compact counterparts. This type also generally has the basic shape of the bluff body to maximize the space volume of the passenger compartment. In terms of aerodynamics, this form results in larger aerodynamic drag due to the occurrence of enormous flow separation in rear parts of the vehicle body creating higher energy consumption of the vehicle. The aerodynamic drag contributes about half of mechanical energy expenditures of vehicles running at average highway speed of around 55 to 60 mph [1].

Ahmed vehicle model is an extremely simplified bluff-body model frequently used as a benchmark in vehicle aerodynamics research. A number of experimental research [2-6] and numerical studies [7-12] have been performed using the Ahmed model. One of the techniques under development to reduce aerodynamic drag on vehicles and to modify the generation of flow separation in the boundary layer on the surface of the vehicle which resulted in the generation of a backflow around the vehicle is the active flow control application. Active control strategies involve the addition of energy which aims to control, either in the form of prevention or inhibiting, the occurrence of flow separation which may lead to backflow on the surface of the vehicle without changing the shape of vehicles [13].

Some active control techniques have been developed and focusing on local intervention in wall turbulence dealing with steady blowing or suction [14-22]. Krentel et.al. modeled a predictive closed-loop actuation approach for one steady blowing excitation configuration [16]. Harinaldi et al. [23] used a modified or reversed Ahmed body equipped with active flow control by blowing and found that the drag reductions achieved by computational and experimental methods were 13.92% and 11.11%. A review has also been elaborated for methods for the application of flow control on a square back car model [24]. This study aimed to analyze the effect of blowing active control incorporating the variations on front geometry towards the reduction aerodynamic drag on vehicle models. Improved reduction of aerodynamic drag can reduce flow separation which in turns will lead to energy efficiency. Comprehension of aerodynamic drag reductions and pressure coefficients are expected to improve the design method of future vehicles.

2. METHODOLOGY

The study investigates drag reduction occurring in a bluff body of van model adapted from Ahmed model, in

Received:
Correspondence to: Dr Rustan Tarakka
Department of Mechanical Engineering,
Jl. Poros Malino, Gowa, Indonesia
E-mail: rustan_tarakka@yahoo.com

which flow streams in reversed direction from the original model or in other names, reversed Ahmed model [23, 25-28]. The van model was equipped with an active control by applying blowing techniques. Reversed Ahmed body model was chosen since it is a good representation of typical forms of popular family van produced by car manufacturer. The van model was investigated in both computational method, or CFD, and experimental method.

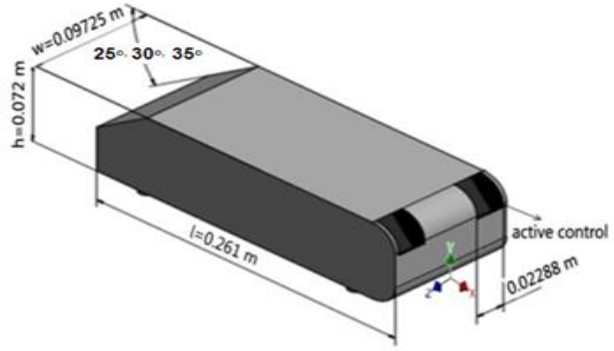

Figure 1. Reversed Ahmed body vehicle model

Figure 1 represents the basic vehicle model employed in the research with a 0.25 geometric ratio to the original Ahmed body model [2]. The vehicle model geometry was defined by its length (l=0.261m), width (w=0.09725 m) and its height (h=0.072 m). In this configuration, the front part of model was inclined with slant angles (θ) of 25°, 30° and 35°relative to the horizontal reference.

The value of viscous drag force and pressure drag force F_d is denoted in the equation (1).

$$F_d = \int \tau_w \sin\theta dS + \int p \cos\theta dS \tag{1}$$

While, drag coefficient C_d is expressed in the equation (2).

$$C_d = \int \frac{\tau_w}{\frac{1}{2}\rho V_\infty^2 S} \sin\theta dS + \frac{\int Cp \cos\theta dS}{S} \tag{2}$$

where $\tau_w = \mu(du/dy)_w$ is the wall shear stress which is assessed from the velocity gradient at the wall and $C_p = (p\text{-}p_\infty)/(\rho V_\infty^2/2)$ is pressure coefficient which is assessed from pressure distribution at the wall.

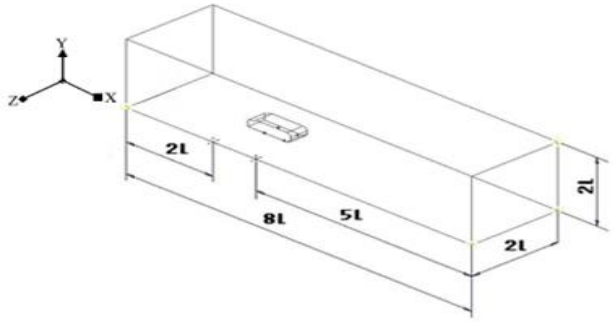

Figure 2. The 3D computational domain

The applied 3D computational domain is as shown in figure 2 denoting dimensions of length (L)=8l, width (W)=2l, and height (H)=2l, where l is the length of model in x-axis. This computation approach utilizes standard k-epsilon turbulence model as described on equation (3) for kinetic energy and equation (4) for dissipation rate.

$$\frac{\partial}{\partial t}(\rho k) + \frac{\partial}{\partial x_i}(\rho k u_i) = \frac{\partial}{\partial x_j}\left[\left(\mu + \frac{\mu_t}{\sigma_k}\right)\frac{\partial k}{\partial x_j}\right] + P_k + P_b - \rho_\epsilon - Y_M + S_k \tag{3}$$

$$\frac{\partial}{\partial t}(\rho \epsilon) + \frac{\partial}{\partial x_i}(\rho \epsilon u_i) = \left[\left(\mu + \frac{\mu_t}{\sigma_\epsilon}\right)\frac{\partial \epsilon}{\partial x_j}\right] + C_{1\epsilon}\frac{\epsilon}{k}(P_k + C_{3\epsilon}P_b) - C_{2\epsilon}\rho\frac{\epsilon^2}{k} + S_\epsilon \tag{4}$$

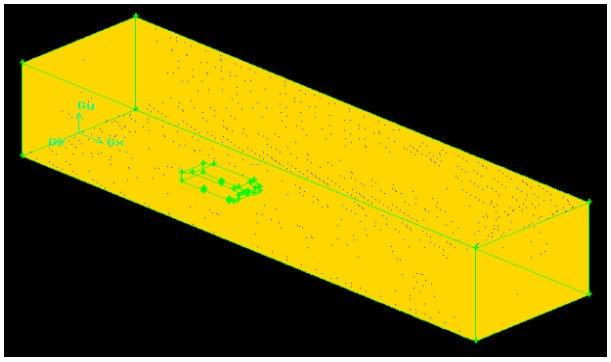

a. Vehicle model with θ=25°

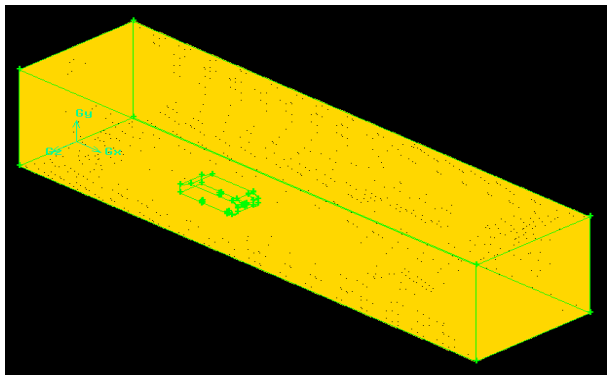

b. Vehicle model with θ=30°

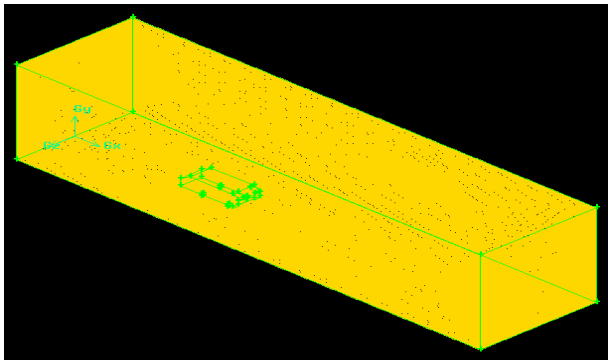

c. Vehicle model with θ=35°

Figure 3. Meshing on models with blowing control

Figure 3 shows the meshing on respective vehicle models with the application of blowing on the rear part of models. The type of meshing was tetra/hybrid element with hexcore type, where the number of mesh volume for the model with θ=25ºwas 2,321,940, while for models with θ=30º and θ=35º the number of mesh were 2,274,917 and 2,319,492 respectively. Inlet velocity of 16.7 m/s is assigned as the boundary condition. Average free stream at upstream region was assumed to be in a steady state and uniform condition. The blowing speed was defined in0.5 m/s. Reynolds number corresponding to the length of the test model was at Re=2.98x10^5. The detailed computational conditions are given in table 1.

Table 1. Description of computational condition

Vehicle model	3D, steady state θ=25º, θ=30º andθ=35º	
Fluid	Air	
Fluid properties	Density Viscosity	1.225 kg/m^3 0.000017894 kg/m-s
Boundary condition without an active flow control	Vehicle model Outlet Inlet Wall	Wall Pressure outlet Velocity inlet Wall
Boundary condition with blowing flow control	Vehicle model Outlet Inlet Wall Blowing1 Blowing2	Wall Pressure outlet Velocity inlet Wall Velocity inlet Velocity inlet
Upstream velocity	16.7 m/s	
Blowing velocity	0.5 m/s	

The tests were conducted in a controlled subsonic wind tunnel supplied with free stream air flow, testing acrylic van model with a 0.25 scale to the original Ahmed body model [2]. The wind tunnel has been calibrated complying manufacturer specification and considering recommendation by several works [29-31]. The van models are classified as models without flow control and models with blowing flow control. The blowing apparatus was configured at the internal part of the body of the model where the flow separation was predicted by computational method to induce a significant drag. The blowing apparatus was operated by using a mini compressor with blowing velocity at 0.5 m/s.

The investigated parameter was the aerodynamic drag force measured by using a load cell. Prior to the main experiments, the load cell was calibrated by using a digital balance. A preliminary measurement was performed to determine the statistical uncertainty of force measurements which was predicted to range at about ± 2%. The setup for the aerodynamic drag force measurement is as shown in figure 4.

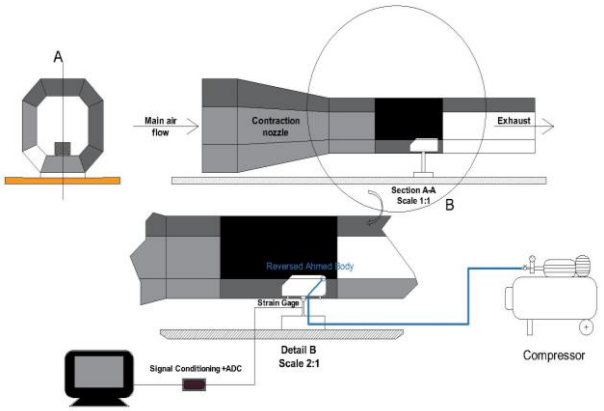

Figure 4. Experimental setup for the aerodynamic drag force measurement

Dimensionless drag coefficient relative to drag force working on the bluff body is defined in the equation (5):

$$C_d = \frac{F_d}{\frac{1}{2}\rho V_\infty^2 S} \tag{5}$$

where, ρ is air density, V_∞ is free stream velocity, S is cross sectional area and F_d is the total drag force working on vehicle models as measured by the load cell.

3. RESULTS AND DISCUSSION

Main results of the research are pressure coefficients and aerodynamic drags which evaluated in terms of reduction in the application of blowing active control. Figure 5 presents contour pathlines coloured by static pressure for models without active flow control for respective front slant angles.

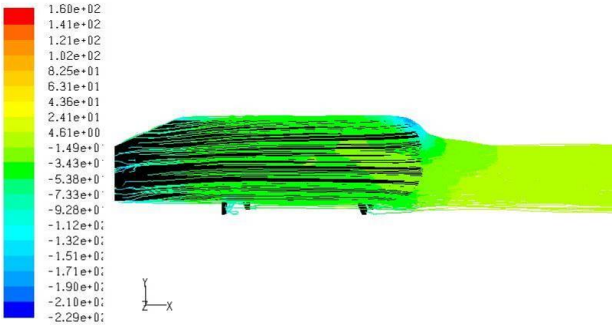

a. Vehicle model with θ=25°

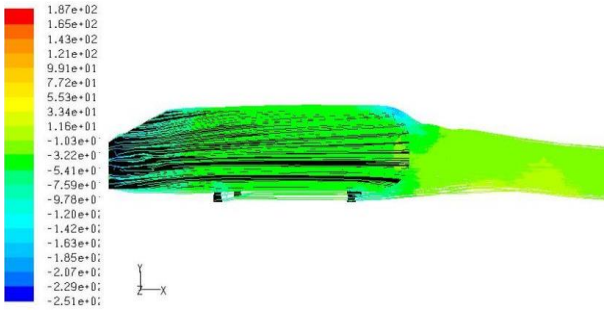

b. Vehicle model with θ=30°

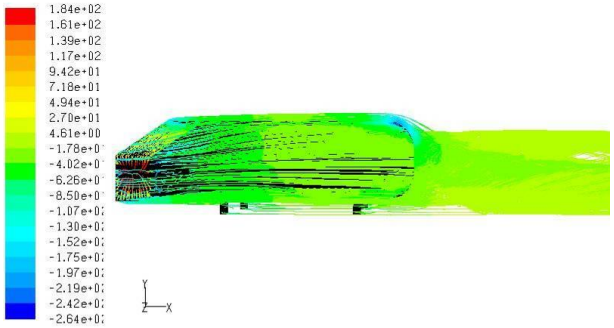

c. Vehicle model with θ=35°

Figure 5. Pathlines colored by static pressure without active flow control

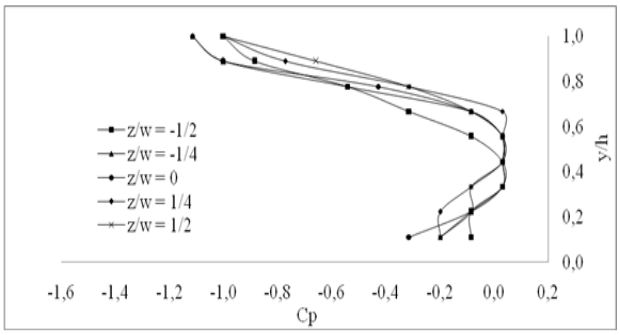

a. Vehicle model with θ=25°

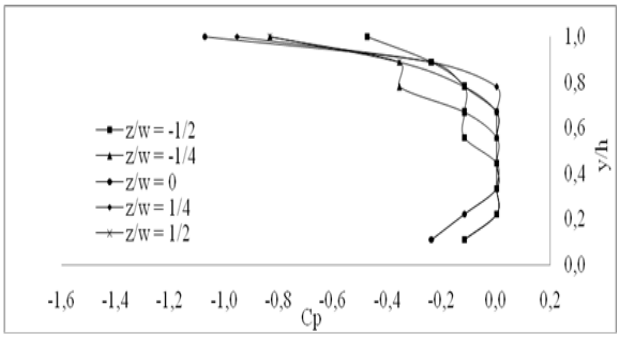

b. Vehicle model with θ=30°

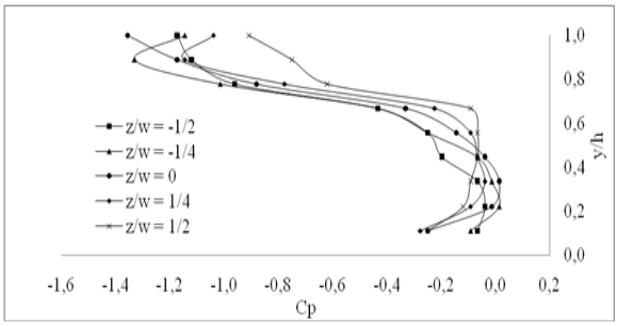

c. Vehicle model with θ=35°

Figure 6. The distribution of pressure coefficients without an active flow control

The relationships of flow characteristics and vehicle's geometric parameters are presented in consecutive figures and tables. The first to be discussed is the expression of the distribution of pressure coefficient C_p in the relation to the so-called y/h ratio which is the ratio of the height of the grid to the height of vehicle model. The second will be the patterns of pressure coefficient distribution on the rear part of vehicle models in regards with z/w parameter, the ratio of width of grid to the width of vehicle models. The first one is shown in figure 6 for vehicle models with slant angle variations (θ) of 25°, 30°and 35°and given upstream velocity of 16.7 m/s.

The minimum values of pressure coefficients on respective test model are presented in table 2 where, as shown in the table 2, the minimum value of pressure coefficients occurs at y/h=1, specifically on the edge of upper side of rear part of respective vehicle models. The highest pressure coefficient is recorded on the vehicle model with a 30° front slant angle as compared to the coefficients on models with 25°and 35°frontal slant angles. It is expected that a flow separation is likely to occur on the rear part of vehicle models, where the separation could induce back flow and therefore can reduce the pressure coefficient. This evidence is in agreement with the opinion of Anderson et al. [32].

Table 2, The minimum value of pressure coefficients without an active flow control

Vehicle model	Pressure coefficient, C_p	y/h	z/w
$\theta=25^0$	-1.1148	1	-1/4 and 0
$\theta=30^0$	-1.0716	1	0
$\theta=35^0$	-1,3556	1	0

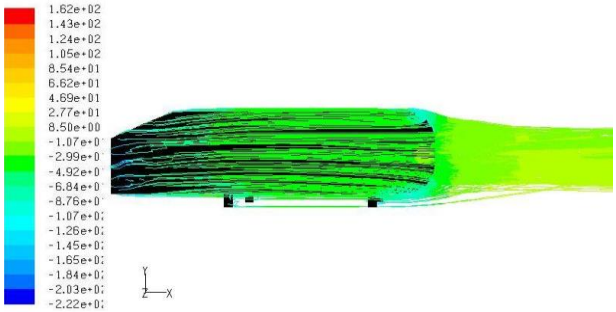

a. Vehicle model with θ = 25°

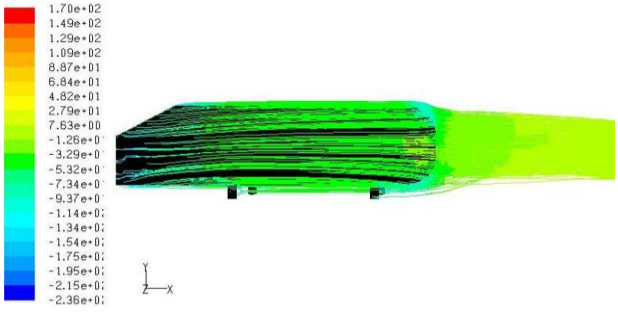

b. Vehicle model with θ = 30°

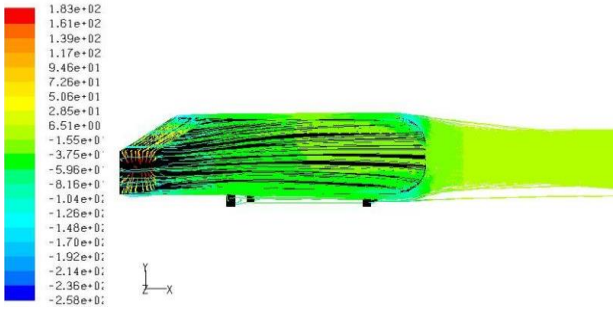

c. Vehicle model with θ = 35°

Figure 7. Pathlines colored by static pressure with blowing flow control

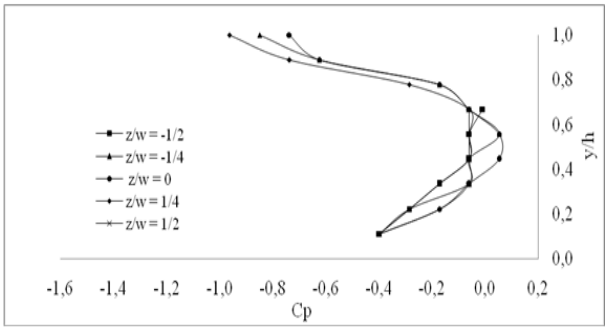

a. Vehicle model with θ = 25°

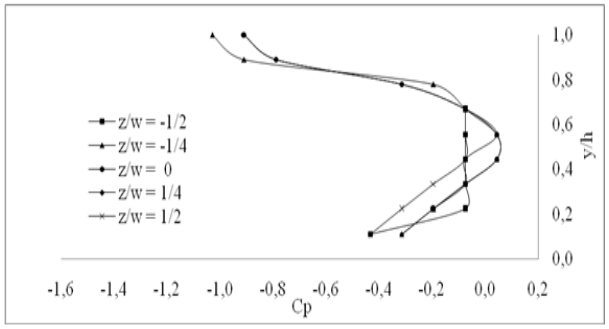

b. Vehicle model with θ = 30°

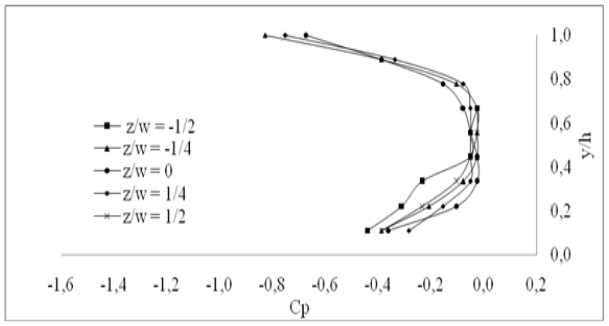

c. Vehicle model with θ = 35°

Figure 8. Pressure coefficient distribution with blowing flow control

The presence of active control in the form of blowing was then evaluated based on the same parameter. Figure 7 presents contour pathlines colored by static pressure for models with the application of blowing active flow control for respective front slant angles. Figure 8 presents the distributions of pressure coefficients for given 16.7 m/s upstream velocity U_o as well as 0.5 m/s blowing velocity U_{bl}; all were applied on vehicle models with frontal slant angles of 25°, 30° and 35° respectively. The figures show that with the application of blowing flow control, the pressure coefficient tends to increase. From around y/h=0.6 to y/h=1, pressure coefficients start to change in a positive direction. This finding shows that on the upper side of the rear part of respective model, pressure coefficient increases. By the application of blowing flow control, the lower pressure stream, and considering the shape factor and friction of air with model's wall can be reduced therefore the flow separation the rear part of the test model can be reduced as well. Table 3 summarizes the minimum values of the pressure coefficient distribution on a 0.5 m/s given blowing velocity U_{bl} and a 16.7 m/s upstream velocity U_o. The table also shows that the smallest pressure coefficient distribution was on the model with a 30° front slant angle when compared to the test model with 25° and 35° slant angles.

Table 3. Minimum values of pressure coefficient with blowing flow control

Vehicle model	Pressure coefficient, C_p	y/h	z/w
$\theta=25^0$	-0.9622	1	1/4
$\theta=30^0$	-1.0285	1	-1/4
$\theta=35^0$	-0.8279	1	-1/4

The effect of additional active control by blowing with U_{bl}=0.5 m/s blowing speed in the reduction of the flow separation at the rear of each vehicle model is shown in table 4. The reduced flow separation gives an effect in the increase of the pressure coefficients on all vehicle models [33].

Table 4. Increasing pressure coefficient with blowing flow control

Vehicle model	Pressure coefficient, C_p		Increasing C_p, (%)
	Without active flow control	With blowing	
$\theta=25^0$	-1.1148	-0.9622	13.69
$\theta=30^0$	-1.0716	-1.0285	4.02
$\theta=35^0$	-1,3556	-0.8279	38.93

The largest value of increasing of pressure coefficient with the addition of blowing active control is on the model with 35° front slant angle gaining a number of percentages of 38.93%.

3.1 The computational method

Table 5 presented the aerodynamic drag coefficients for computational approach on the vehicle models with frontal slant angle of θ=25°, θ=30° and θ=35° both for normal treatment (without flow control) and with the addition blowing flow control with blowing speed U_{bl} of 0.5 m/s and upstream velocity U_o of 16.7 m/s.

Table 5. Aerodynamic drag coefficient and aerodynamic drag reduction by computational method

Vehicle model	Aerodynamic drag coefficient, C_d		Aerodynamic drag reduction, %
	without active flow control	with blowing	
$\theta=25^0$	1.7752	1.5639	11.90
$\theta=30^0$	1.6709	1.5699	6,04
$\theta=35^0$	1.7556	1.4953	14.81

Table 5 gives information that, in vehicle model without active control, the smallest aerodynamic drag coefficient is obtained in model with a 30° slant angle with the value of 1.6709 while on the models with 25°and 35° front slant angles, aerodynamic drag coefficients were 1.7752 and 1.7556 respectively. It is shown that the aerodynamic drag coefficients on each model were decreasing as the effect of the additional blowing active control while the smallest drag coefficient occurred in the model with θ=35°where the value of 1.4953. For models with θ=25° and θ=30°, the

aerodynamic drag coefficients were 1.5639and 1.5699 respectively.

From the table 5 also, the largest reduction of aerodynamic drag as the effect of blowing flow control occurs on vehicle model with θ of 35° on a given 0.5 m/s blowing velocity U_{bl} and 16.7 m/s upstream velocity U_o with the reduction percentage was 14.81% . For the vehicle models with slant angles of 25°and 30°, the reduction were 11.90% and 6.04% respectively, as shown in table 5. The aerodynamic drag value on vehicle model with front slant angle 35° is capable to increase pressure coefficient on rear part of vehicle model for up to 38.93% as the effect of blowing flow control. The increasing of pressure coefficient on rear parts of vehicle models can decrease the aerodynamic drag. Results obtained from the research have confirmed the results of other researchers [16, 18, 23, 26, 27] where the application of active control by blowing can reduce aerodynamic drag on vehicle models.

3.2 The experimental method

Table 6 presents the aerodynamic drag coefficients obtained from experimental method on three vehicle models, which have similar geometric parameters to the model used for computational method.

Table 6. Aerodynamic drag coefficient and aerodynamic drag reduction by experimental method

Vehicle model	Aerodynamic drag coefficient, C_d		Aerodynamic drag reduction, %
	without active flow control	with blowing	
$\theta=25^0$	1.6237	1.4480	10.82
$\theta=30^0$	1.5173	1.4313	5.67
$\theta=35^0$	1.5655	1.3747	12.54

Table 6 gives the information that for models without flow control, the smallest aerodynamic drag coefficients occurs in the 30° front slant angle vehicle modelwith 1.5173 value as for models with θ=25°and θ=35°, the aerodynamic drag coefficients were 1.6237 and 1.5655 respectively. Additional blowing flow control for all models gives reduction of aerodynamic drag coefficients while the smallest aerodynamic drag coefficients occurred in the model with a 35°front slant angle with the value of 1.3747% and 1.4480% as well as 1.4313% for vehicle models with θ=25° and θ=30°.

From the table 6 also, it is obvious that the smallest reduction of aerodynamic drag by active control with blowing speed U_{bl} of 0.5 m/s and upstream velocity U_o of 16.7 m/s occurred on the model with θ=35° giving the reduction of 12.54% while on models with θ=25° dan θ=30° the reductions were 10.82% and 5.67% respectively.

The comparison of aerodynamic drag coefficients for vehicle models with θ=25°, θ=30°and θ=35° front slant angles obtained from both computational method as well as experimental method are shown on tables 7, 8 and 9 respectively.

Table 7 contains the comparison of aerodynamic drag coefficient for vehicle model with slant angle θ=25° from computational and experimental methods. It is shown that the aerodynamic drags coefficients from the two methods on models without flow control differ in about 8.53%, as for models with a 0.5 m/s blowing flow control, the two methods result a 7.41% difference in the value of aerodynamic drag coefficient. The table 7 also informs that there is a 1.08% slight difference in the reduction of aerodynamic drag coefficient for the two methods.

Table 7. Aerodynamic drag coefficient (C_d) for vehicle model with $\theta=25^0$

Description	Aerodynamic drag coefficient, (C_d)		Aerodynamic drag coefficient (C_d) reduction (%)
	without active flow control	with blowing	
Computational	1.7752	1.5639	11.90
Experimental	1.6237	1.4480	10.82
Difference	8.53%	7.41%	1.08

Table 8 shows the comparison of aerodynamic drag coefficients from both computational and experimental approaches for vehicle model with slant angle of θ=30°.The coefficients of aerodynamic drag of the two methods for models without flow control differ on 9.19% differences. For vehicle models with blowing flow control at blowing speed of 0.5 m/s, the two methods give 8.83% difference in aerodynamic drag coefficient values. The table 8 also shows that the reduction of aerodynamic drag coefficients between computational and experimental methods differ on only 0.37%.

Table 8. Aerodynamic drag coefficient (C_d) for vehicle model with $\theta=30^0$

Description	Aerodynamic drag coefficient, (C_d)		Aerodynamic drag coefficient (C_d) reduction (%)
	without active flow control	with blowing	
Computational	1.6709	1.5699	6.04
Experimental	1.5173	1.4313	5.67
Difference	9.19%	8.83%	0.37

Table 9. Aerodynamic drag coefficient (Cd) for vehicle model with θ=350

Description	Aerodynamic drag coefficient, (C_d)		Aerodynamic drag coefficient (C_d) reduction (%)
	without active flow control	with blowing	
Computational	1.7556	1.4953	14.81
Experiment	1.5655	1.3706	12.54
Difference	10.82%	8.34%	2.27

Aerodynamic drag coefficients obtained from computational and experimental methods for θ=35° model are listed in table 9. For models without flow control, the aerodynamic drag coefficients of the two methods have 10.82% differences. On vehicle models

with active blowing flow control at blowing speed of 0.5 m/s, the two methods give 8.34% difference in aerodynamic drag coefficient values. The table 9 also shows that the reductions of aerodynamic drag coefficients of the two methods differ about 2.27%.

4. CONCLUSION

Based on the results of pressure coefficients and drag reduction on reversed Ahmed vehicle models with front slant angles (θ) of 25°, 30° and 35° as well as the application of blowing flow control, some conclusion can be drawn. It is obvious that the active flow control by blowing and variations on front geometry provide significant impact to the increasing of pressure coefficients and reduction of aerodynamic drag. The most significant increase on pressure coefficients occurs on vehicle model with the 35° front slant angle, gaining 38.93% value, where pressure coefficients with and without blowing flow control reach -0.8279 and -1.3556, respectively. In terms of aerodynamic drag reduction, vehicle model with the 35° front slant angle also gains the value of 14.81 and 12.54 for computational and experimental methods, while the reductions of aerodynamic drag coefficients of the two approaches have 2.27% difference.

ACKNOWLEDGEMENTS

The research was funded by the Ministry of Research, Technology and Higher Education, The Republic of Indonesia, through University Excellence Scheme F.Y 2018, with Research Contract No. : 1579/UN4.21/PL.00.00/2018, dated March 21th 2018.

REFERENCES

[1] Agarwal, R.K."Sustainable ground transportation – review of technologies, challenges and opportunities", International Journal of Energy and Environment, Vol. 4, No.6, pp.1061-10782013, 2013.

[2] Ahmed, S., Ramm, G., Faltin, G."Some Salient Features Of The Time-Averaged Ground Vehicle Wake", SAE Technical Paper 840300, 1984.

[3] Sims-Williams, D., Dominy, R. "Experimental Investigation into Unsteadiness and Instability in Passenger Car Aerodynamics", SAE Technical Paper 980391, 1998.

[4] Bayraktar, I., Landman, D., Baysal, O. "Experimental and Computational Investigation of Ahmed Body for Ground Vehicle Aerodynamics", SAE Technical Paper 2001-01-2742, 2001.

[5] Joseph, P., Amandolese, X., Edouard, C. Aider, J. "Flow control using MEMS pulsed micro-jets on the Ahmed body", Experiment in Fluids, Vol. 54, No. 1, 1442, 2013.

[6] Lienhart, H., Becker, S. "Flow and Turbulence Structure in the Wake of a Simplified Car Model", SAE Technical Paper 2003-01-0656, 2003,

[7] Han, T. "Computational analysis of three-dimensional turbulent flow around a bluff body in ground proximity", AIAA Journal, Vol. 27, No.9, 1989, pp. 1213-1219.

[8] Basara, B., Przulj, V., Tibaut, P. "On the Calculation of External Aerodynamics: Industrial Benchmarks", SAE Technical Paper 2001-01-0701, 2001.

[9] Basara, B. "Numerical simulation of turbulent wakes around a vehicle", in: *ASME Fluid Engineering Division Summer Meeting FEDSM99-7324*. San Francisco, USA, 1999.

[10] Basara, B., Alajbegovic, A. "Steady state calculations of turbulent flow around Morel body". in: *7th International Symposium of Flow Modelling and Turbulence Measurements*, Taiwan, 1998, pp. 1–8

[11] Gilliéron, P.,Chometon, F. "Modeling of stationary three-dimensional separated air flows around an Ahmed reference model", in : *ESAIM, Proceeding of Third International Workshop on Vortex Flows and Related Numerical Methods*, 7, 1999, pp. 173–182.

[12] Kapadia, S., Roy, S., Vallero, M., Wurtzler, K., Forsythe J. "Detached-Eddy Simulation over a Reference Ahmed Car Model", in: Friedrich, R., Geurts, B.J., Métais, O. (eds*) Direct and Large-Eddy Simulation V*. ERCOFTAC Series, 9. Springer, Dordrecht, 2004, pp 481-488.

[13] Conan, B., Anthoine, J., Planquart, P. "Experimental aerodynamic study of a car-type bluff body", Experiments in Fluids, Vol. 50, No. 5, pp.1273-1284, 2010.

[14] Krogstad, P.A., Kourakine, A. "Some effects of localized injection on the turbulence structure in a boundary layer", Physics of Fluids, Vol. 12, No.11, pp. 2990-2999, 2000.

[15] Park, J., Choi, H. "Effects of uniform blowing through blowing or suction from a spanwise slot on a turbulent boundary layer flow", Physics of Fluids, Vol. 11, No. 10, pp. 3095–3105, 1999.

[16] Krentel D., Muminovic R., Brunn A., Nitsche W., King R. "Application of Active Flow Control on Generic 3D Car Models". in: King R. (eds) *Active Flow Control II. Notes on Numerical Fluid Mechanics and Multidisciplinary Design*, 108. Springer, Berlin-Heidelberg, Germany, 2010, pp. 223-239.

[17] Heinemann, T., Springer, M., Lienhart, H. "Active flow control on a 1:4 car model", Experiments in Fluids, Vol. 55, No. 5, 1738, 2014.

[18] Mestiri, R., Ahmed-Bensoltane, A., Keirsbulck, L., Aloui, F.,Labraga, L. "Active Flow Control at the Rear End of a Generic Car Model Using Steady Blowing", Journal of Applied Fluid Mechanics, Vol. 7, No. 4, pp. 565-571, 2014.

[19] Tounsi, N., Mestiri, R., Keirsbulck, L., Oualli, H., Hanchi, S., Aloui, F."Experimental Study of Flow Control on Bluff Body using Piezoelectric Actuators" , Journal of Applied Fluid Mechanics , Vol. 9, No. 2, pp. 827-838, 2016.

[20] Tian, J., Zhang, Y., Zhu, H., Xiao, H."Aerodynamic drag reduction and flow control of Ahmed body with flaps", Advances in Mechanical Engineering, Vol. 9, No.7, pp. 1–17, 2017.

[21] Shadmani, S., Mousavi-Nainiyan, S.M., Ghasemiasl, R.,Mirzaei, M., Pouryoussefi, S.G. "Experimental Study of Flow Control Over an Ahmed Body Using Plasma Actuator", Mechanics and Mechanical Engineering, Vol. 22, No. 1, pp. 239–251, 2018.

[22] Prakash, B., Bergada, J.M., Mellibovsky, F. "Three Dimensional Analysis of Ahmed Body Aerodynamic Performance Enhancement using Steady Suction and Blowing Flow Control Techniques", in : *Tenth International Conference on Computational Fluid Dynamics (ICCFD10)*, 2018. Barcelona, Spain.

[23] Harinaldi, Budiarso, Tarakka, R., Simanungkalit, S.P. "Effect of Active Control by Blowing to Aerodynamic Drag of Bluff Body Van Model", International Journal of Fluid Mechanics Research, Vol. 40, No.4, pp. 312-323, 2013.

[24] Julian, J., Karim, R.F., Budiarso, Harinaldi, "Review: Flow Control on a Squareback Model" International Review of Aerospace Engineering (IREASE), Vol. 10, No. 4, pp. 230-239, 2017.

[25] Harinaldi, Budiarso, Warjito, Kosasih, E.A., Tarakka, R., Simanungkalit, S.P. "Active technique by suction to control the flowstructure over a van model", Journal of Engineering and Applied Science, Vol. 7, No. 2, pp.215-222, 2012.

[26] Harinaldi, Budiarso, Tarakka, R., Simanungkalit, S.P. "Computational Analysis of Active Flow Control to Reduce Aerodynamics Drag on a Van Model", International Journal of Mechanical & Mechatronics Engineering IJMME-IJENS, Vol. 11, No. 3, pp. 24-30, 2011

[27] Tarakka, R., Jalaluddin, Mire, B., Umar, M.N. "Effect of Turbulence Model In Computational Analysis of Active Flow Control on Aerodynamic Drag of Bluff Body Van Model", International Journal of Applied Engineering Research, Vol. 10, No. 1, pp. 207-219, 2015.

[28] Tarakka, R., Salam, N., Jalaluddin, Ihsan, M. "Active Flow Control by Suction on Vehicle Models with Variations on Front Geometry", International Review of Mechanical Engineering, Vol. 12, No. 2, 2018, pp. 128-134.

[29] Plint and Partners, Manual of Educational Wind Tunnel, England, 1982

[30] Ocokoljić, G., Damljanović, D., Vuković, Đ., Rašuo, B. "Contemporary Frame of Measurement and Assessment of Wind-Tunnel Flow Quality in a Low-Speed Facility", FME Transactions, Vol. 46, No. 4, pp. 429-442, 2018

[31] Ocokoljić, G., Damljanović, D., Rašuo, B., Isaković, J. "Testing of a Standard Model in the VTI's Largesubsonic Wind-tunnel Facility to Establish Users' Confidence", FME Transactions, Vol. 42, No. 3, pp. 212-218, 2014

[32] Anderson, J.D. "Fundamental of Aerodynamics" 3rd ed., McGraw-Hill, Singapore, 2001.

[33] Sphon, A., Gilliéron, P. "Flow separations generated by simplified geometry of an automotive vehicle", in: *IUTAM Symposium: Unsteady separated flows*, 2002, Toulouse, France.

NOMENCLATURE

Cd	drag coefficient
Cp	pressure coefficient
Fd	pressure drag force [N]
h	height of test model [m]
l	length of test model [m]
ρ	density [kg/m^3]
θ	front slant angle [^{o}]
Re	Reynolds number
S	cross section area [m^2]
τ_w	wall shear stress [N/m^2]
U_{bl}	blowing velocity [m/s]
U_o	upstream velocity [m/s]
μ	viscosity [N.s/m^2]
w	width of test model [m]

4. Permintaan informasi perkembangan artikel ke FME Transactions (6 Maret 2019)

Inquiry for Manuscript ID FME-018-353 3

Rustan Tara... /Journal ...

Rustan Tarakka <rustan_tarakka@yahoo.com>
To: brasuo@mas.bg.ac.rs

Wed, Mar 6, 2019 at 7:08 AM

Dear Prof. Bosko Rasuo,
Editor of FME Transactions
Faculty of Mechanical Engineering
University of Belgrade

We have submitted our paper to the Manuscript ID FME-018-353 "Effect of blowing flow control and front geometry towards the reduction of aerodynamic drag on vehicle models" authored by Rustan Tarakka et al. and has been submitted for the revision on December 7th 2018. Herewith, I am asking information regarding any development about the paper, whether there are any further revision.

I hope that the paper has a chance to be published in your respected journal. Thank you very much for your kind attention.
Sincerely yours,

Dr. Rustan Tarakka
Dept. of Mechanical engineering
Hasanuddin University

5. Informasi artikel telah accepted di FME Transactions (7 Maret 2019)

Bosko Rasuo <brasuo@mas.bg.ac.rs>
To: Rustan Tarakka

Thu, Mar 7, 2019 at 2:06 AM

Dear colleague Rustan Tarakka,

I am pleased to inform you that your paper, ID: FME-18-353, titled: "Effect of blowing flow control and front geometry towards the reduction of aerodynamic drag on vehicle models" has been accepted for publication in FME Transactions journal.

Thank you for submitting your work to FME Transactions.

Yours sincerely,

Prof. Bosko Rasuo, Editor of FME Transactions

Clarivate Analytics
Web of Science™

Show original message

6. Permintaan informasi waktu publish artikel ke FME Transactions (27 Maret 2019)

Inquiry for Manuscript ID FME-018-353 3

Rustan Tara... /Journal ...

Rustan Tarakka <rustan_tarakka@yahoo.com>
To: Bosko Rasuo

Wed, Mar 27, 2019 at 10:06 AM

Dear Prof. Bosko Rasuo,
Editor of FME Transactions
Faculty of Mechanical Engineering
University of Belgrade

We are very delighted to learn that our Manuscript ID FME-018-353 "Effect of blowing flow control and front geometry towards the reduction of aerodynamic drag on vehicle models" has been accepted for publication in your esteemed journal. We express our gratitude to you and fellow editors for the acceptance.

We will also very glad if you could inform us, if possible, about when will be the publication of the volume where our paper is included. Thank you very much for your kind attention.

Sincerely yours,

Dr. Rustan Tarakka
Dept. of Mechanical Engineering
Hasanuddin University

7. Informasi waktu publish artikel di FME Transactions (28 Maret 2019)

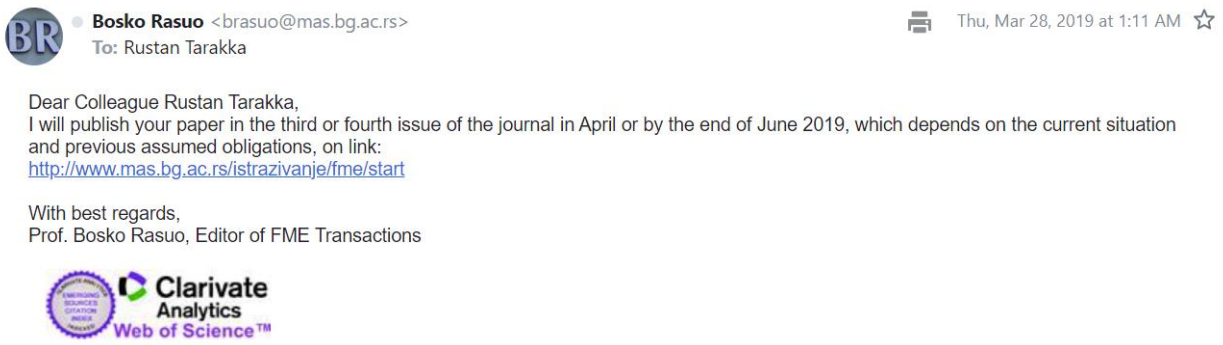

Bosko Rasuo <brasuo@mas.bg.ac.rs>
To: Rustan Tarakka

Thu, Mar 28, 2019 at 1:11 AM

Dear Colleague Rustan Tarakka,
I will publish your paper in the third or fourth issue of the journal in April or by the end of June 2019, which depends on the current situation and previous assumed obligations, on link:
http://www.mas.bg.ac.rs/istrazivanje/fme/start

With best regards,
Prof. Bosko Rasuo, Editor of FME Transactions

Clarivate Analytics
Web of Science™

8. Informasi publish artikel di FME Transaction (28 Juni 2019)

Post publication comments for ID FME-018-353 — Rustan Tara... /FME

Rustan Tarakka <rustan_tarakka@yahoo.com> — Fri, Jun 28, 2019 at 10:29 AM
To: Bosko Rasuo

Dear Prof. Bosko Rasuo,
Editor of FME Transactions
Faculty of Mechanical Engineering
University of Belgrade

We are happy to learn that our paper ID FME-018-353 Effect of blowing flow control and front geometry towards the reduction of aerodynamic drag on vehicle models" authored by Rustan Tarakka et al. has been published in Volume 47 issue 3 on April 2019 and we thank you very much.

However, we would like to inform about some issues regarding the numbering for Figure 3 in the paper (numbered in a, b, c) which are still red colored. We hope that it can be resolved.

Thank you very much for your kind attention.
Sincerely yours

Dr. Rustan Tarakka
Dept. of Mechanical engineering
Hasanuddin University

Effect of Blowing Flow Control and Front Geometry Towards the Reduction of Aerodynamic Drag on Vehicle Models

Rustan Tarakka
Assistant Professor
Hasanuddin University
Department of Mechanical Engineering
Indonesia

Nasaruddin Salam
Professor
Hasanuddin University
Department of Mechanical
Indonesia

Jalaluddin
Associate Professor
Hasanuddin University
Department of Mechanical Engineering
Indonesia

Muhammad Ihsan
Lecturer
Sekolah Tinggi Teknik Baramuli
Department of Civil Engineering
Indonesia

This paper presents analyses of the effect of blowing flow control and variations on front geometry towards the reduction of aerodynamic drag on vehicle models. Blowing flow control is an alternative measure in modifying the onset of flow separation in the boundary layer on the surface of the vehicle. The modification is expected to reduce the dominating influence of the separation area on the total drag. Conducted in computational and experimental approaches, the research investigated the effect of frontal slant angle variations (θ) of 25°, 30° and 35° towards the reduction of aerodynamic drag on vehicle models on the application of blowing flow control with upstream and blowing speed of 16.7 m/s and 0.5 m/s, respectively. Load cells were used in the experimental method to validate the reduction of aerodynamic drag obtained from computational method. It is indicated that the effects of blowing flow control and variations on front geometry are significant in the increasing on pressure coefficients and the reduction of aerodynamic drag on vehicle models. The largest increase on pressure coefficients of 38.93% is indicated on the vehicle model with θ=35°, while the largest reduction of aerodynamic drag occurred on the same model with the values of 14.81 and 12.54 for computational and experimental methods, respectively.

Keywords: *active flow control, aerodynamic drag reduction, blowing, front geometry, vehicle model.*

1. INTRODUCTION

As one of the most preferred types of general vehicles, family car in the form of multi-purpose van (MPV) has both advantages and drawbacks. Of the drawbacks, one typical character is the demand of relatively larger capacity engine which means larger fuel consumption than its more compact counterparts. This type also generally has the basic shape of the bluff body to maximize the space volume of the passenger compartment. In terms of aerodynamics, this form results in larger aerodynamic drag due to the occurrence of enormous flow separation in rear parts of the vehicle body creating higher energy consumption of the vehicle. The aerodynamic drag contributes about half of mechanical energy expenditures of vehicles running at average highway speed of around 55 to 60 mph [1].

Ahmed vehicle model is an extremely simplified bluff-body model frequently used as a benchmark in vehicle aerodynamics research. A number of experimental research [2-6] and numerical studies [7-12] have been performed using the Ahmed model. One of the techniques under development to reduce aerodynamic drag on vehicles and to modify the generation of flow separation in the boundary layer on the surface of the vehicle which resulted in the generation of a backflow around the vehicle is the active flow control application. Active control strategies involve the addition of energy which aims to control, either in the form of prevention or inhibiting, the occurrence of flow separation which may lead to backflow on the surface of the vehicle without changing the shape of vehicles [13].

Some active control techniques have been developed and focusing on local intervention in wall turbulence dealing with steady blowing or suction [14-22]. Krentel et al. modeled a predictive closed-loop actuation approach for one steady blowing excitation configuration [16]. Harinaldi et al. [23] used a modified or reversed Ahmed body equipped with active flow control by blowing and found that the drag reductions achieved by computational and experimental methods were 13.92% and 11.11%. A review has also been elaborated for methods for the application of flow control on a square back car model [24]. This study aimed to analyze the effect of blowing active control incorporating the variations on front geometry towards the reduction aerodynamic drag on vehicle models. Improved reduction of aerodynamic drag can reduce flow separation which in turns will lead to energy efficiency. Comprehension of aerodynamic drag reductions and pressure coefficients are expected to improve the design method of future vehicles.

2. METHODOLOGY

The study investigates drag reduction occurring in a bluff body of van model adapted from Ahmed model, in

Received: November 2018, Accepted: March 2019
Correspondence to: Dr Rustan Tarakka
Department of Mechanical Engineering,
Jl. Poros Malino, Gowa, Indonesia
E-mail: rustan_tarakka@yahoo.com
doi: 10.5937/fmet1903552T

which flow streams in reversed direction from the original model or in other names, reversed Ahmed model [23, 25-28]. The van model was equipped with an active control by applying blowing techniques. Reversed Ahmed body model was chosen since it is a good representation of typical forms of popular family van produced by car manufacturer. The van model was investigated in both computational method, or CFD, and experimental method.

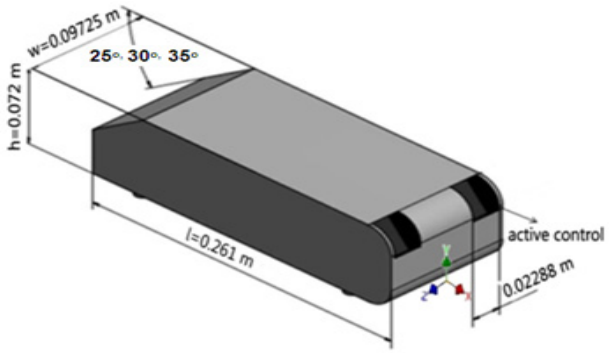

Figure 1. Reversed Ahmed body vehicle model

Figure 1 represents the basic vehicle model employed in the research with a 0.25 geometric ratio to the original Ahmed body model [2]. The vehicle model geometry was defined by its length (l=0.261m), width (w=0.09725 m) and its height (h=0.072 m). In this configuration, the front part of model was inclined with slant angles (θ) of 25°, 30° and 35°relative to the horizontal reference.

The value of viscous drag force and pressure drag force F_d is denoted in the equation (1).

$$F_d = \int \tau_w \sin\theta dS + \int p\cos\theta dS \tag{1}$$

while, drag coefficient C_d is expressed in the equation (2).

$$C_d = \int \frac{\tau_w}{\frac{1}{2}\rho V_\infty^2 S}\sin\theta dS + \frac{\int Cp\cos\theta dS}{S} \tag{2}$$

where $\tau_w = \mu(du/dy)_w$ is the wall shear stress which is assessed from the velocity gradient at the wall and $C_p = (p-p_\infty)/(\rho V_\infty^2/2)$ is pressure coefficient which is assessed from pressure distribution at the wall.

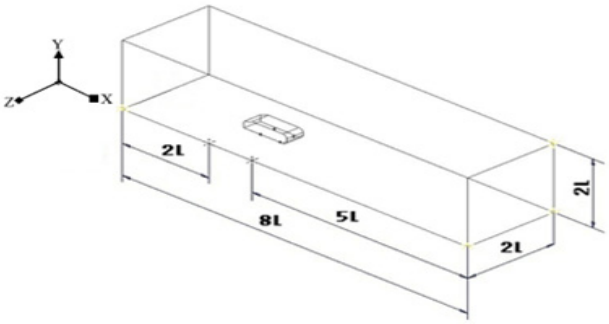

Figure 2. The 3D computational domain

The applied 3D computational domain is as shown in figure 2 denoting dimensions of length (L)=8l, width (W)=2l, and height (H)=2l, where l is the length of model in x-axis. This computation approach utilizes standard k-epsilon turbulence model as described on equation (3) for kinetic energy and equation (4) for dissipation rate.

$$\frac{\partial}{\partial t}(\rho k)+\frac{\partial}{\partial x_i}(\rho k u_i)=\frac{\partial}{\partial x_j}\left[\left(\mu+\frac{\mu_t}{\sigma_k}\right)\frac{\partial k}{\partial x_j}\right]+ \tag{3}$$
$$+P_b-\rho_\varepsilon+Y_M+S_k$$

$$\frac{\partial}{\partial t}(\rho\varepsilon)+\frac{\partial}{\partial x_i}(\rho\varepsilon u_i)=\left[\left(\mu+\frac{\mu_t}{\sigma_\varepsilon}\right)\frac{\partial\varepsilon}{\partial x_j}\right]+ \tag{4}$$
$$+c_{1\varepsilon}\frac{\varepsilon}{k}(P_k+C_{3\varepsilon}P_b)-C_{2\varepsilon}\rho\frac{\varepsilon^2}{k}+S_\varepsilon$$

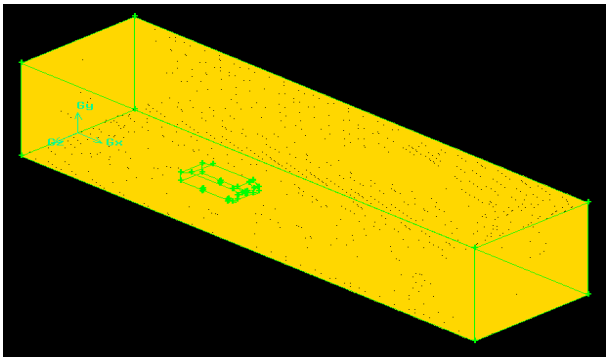

a. Vehicle model with θ=25°

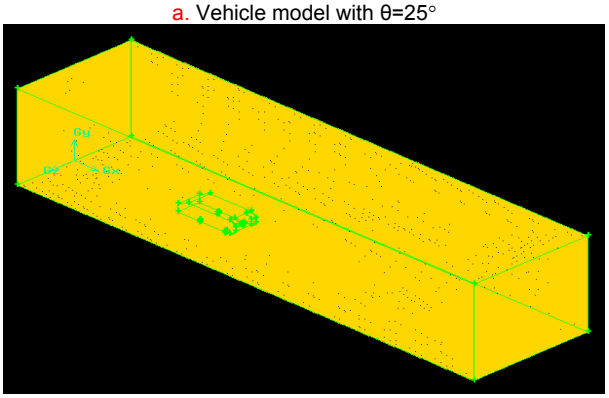

b. Vehicle model with θ=30°

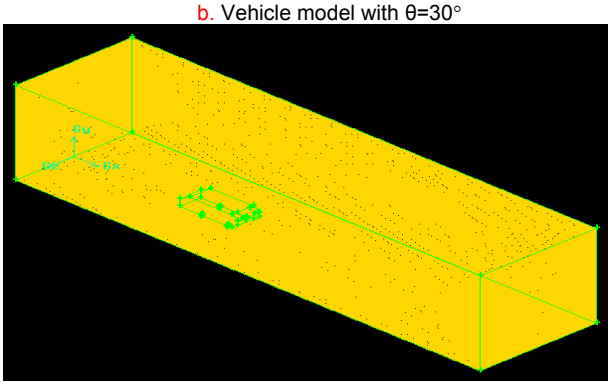

c. Vehicle model with θ=35°

Figure 3. Meshing on models with blowing control

Figure 3 shows the meshing on respective vehicle models with the application of blowing on the rear part of models. The type of meshing was tetra/hybrid element with hexcore type, where the number of mesh volume for the model with θ=25°was 2,321,940, while for models with θ=30° and θ=35° the number of mesh were 2,274,917 and 2,319,492 respectively. Inlet velocity of 16.7 m/s is assigned as the boundary condition. Average free stream at upstream region was

assumed to be in a steady state and uniform condition. The blowing speed was defined in0.5 m/s. Reynolds number corresponding to the length of the test model was at Re=2.98x10^5. The detailed computational conditions are given in table 1.

Table 1. Description of computational condition

Vehicle model	3D, steady state θ=25^o, θ=30^o andθ=35^o	
Fluid	Air	
Fluid properties	Density Viscosity	1.225 kg/m^3 0.000017894 kg/m-s
Boundary condition without an active flow control	Vehicle model Outlet Inlet Wall	Wall Pressure outlet Velocity inlet Wall
Boundary condition with blowing flow control	Vehicle model Outlet Inlet Wall Blowing1 Blowing2	Wall Pressure outlet Velocity inlet Wall Velocity inlet Velocity inlet
Upstream velocity	16.7 m/s	
Blowing velocity	0.5 m/s	

The tests were conducted in a controlled subsonic wind tunnel supplied with free stream air flow, testing acrylic van model with a 0.25 scale to the original Ahmed body model [2]. The wind tunnel has been calibrated complying manufacturer specification and considering recommendation by several works [29-31]. The van models are classified as models without flow control and models with blowing flow control. The blowing apparatus was configured at the internal part of the body of the model where the flow separation was predicted by computational method to induce a significant drag. The blowing apparatus was operated by using a mini compressor with blowing velocity at 0.5 m/s.

The investigated parameter was the aerodynamic drag force measured by using a load cell. Prior to the main experiments, the load cell was calibrated by using a digital balance. A preliminary measurement was performed to determine the statistical uncertainty of force measurements which was predicted to range at about ± 2%. The setup for the aerodynamic drag force measurement is as shown in figure 4.

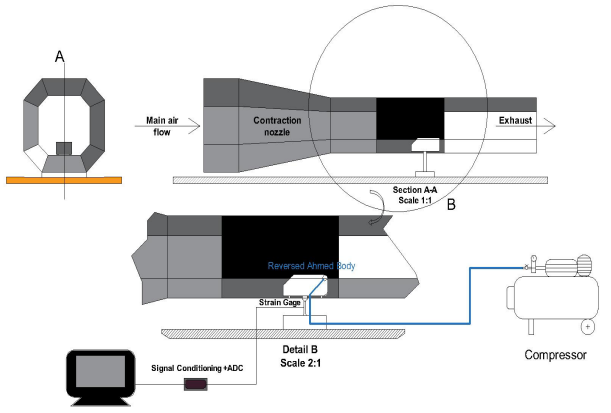

Figure 4. Experimental setup for the aerodynamic drag force measurement

Dimensionless drag coefficient relative to drag force working on the bluff body is defined in the equation (5):

$$C_d = \frac{F_d}{\frac{1}{2}\rho V_\infty^2 S} \tag{5}$$

where, ρ is air density, V_∞ is free stream velocity, S is cross sectional area and F_d is the total drag force working on vehicle models as measured by the load cell.

3. RESULTS AND DISCUSSION

Main results of the research are pressure coefficients and aerodynamic drags which evaluated in terms of reduction in the application of blowing active control. Figure 5 presents contour pathlines coloured by static pressure for models without active flow control for respective front slant angles.

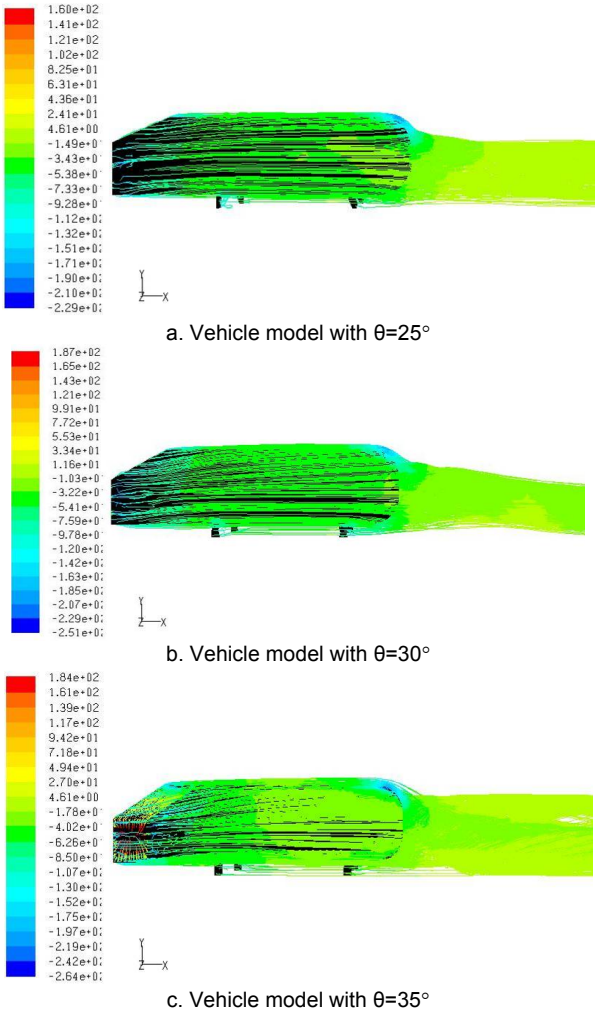

Figure 5. Pathlines colored by static pressure without active flow control

The relationships of flow characteristics and vehicle's geometric parameters are presented in consecutive figures and tables. The first to be discussed is the expression of the distribution of pressure coefficient C_p in the relation to the so-called y/h ratio which is the ratio of the height of the grid to the height of vehicle model. The second will be the patterns of pressure coefficient distribution on the rear part of vehicle models in

regards with z/w parameter, the ratio of width of grid to the width of vehicle models. The first one is shown in figure 6 for vehicle models with slant angle variations (θ) of 25°, 30° and 35° and given upstream velocity of 16.7 m/s.

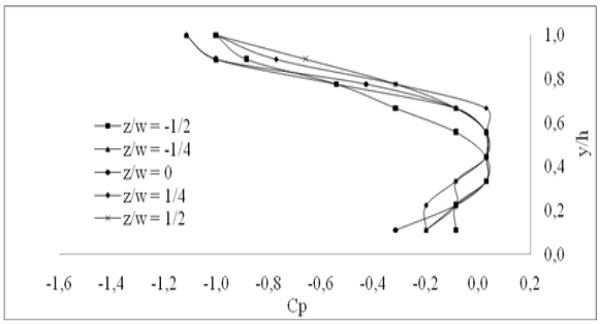

Vehicle model with θ=25°

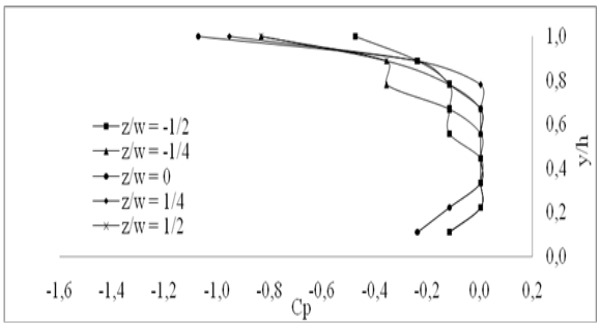

Vehicle model with θ=30°

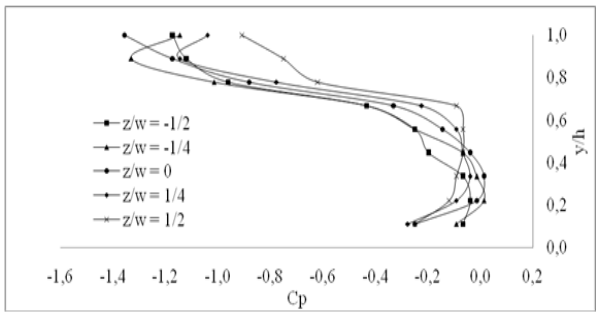

Vehicle model with θ=35°

Figure 6. The distribution of pressure coefficients without an active flow control

The minimum values of pressure coefficients on respective test model are presented in table 2 where, as shown in the table 2, the minimum value of pressure coefficients occurs at y/h=1, specifically on the edge of upper side of rear part of respective vehicle models. The highest pressure coefficient is recorded on the vehicle model with a 30° front slant angle as compared to the coefficients on models with 25°and 35°frontal slant angles. It is expected that a flow separation is likely to occur on the rear part of vehicle models, where the separation could induce back flow and therefore can reduce the pressure coefficient. This evidence is in agreement with the opinion of Anderson et al. [32].

Table 2, The minimum value of pressure coefficients without an active flow control

Vehicle model	Pressure coefficient, C_p	y/h	z/w
$\theta=25^0$	-1.1148	1	-1/4 and 0
$\theta=30^0$	-1.0716	1	0
$\theta=35^0$	-1,3556	1	0

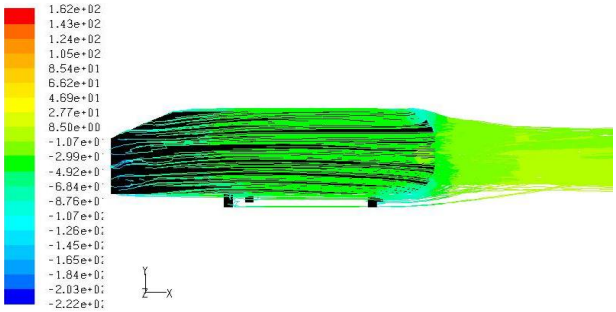

Vehicle model with θ = 25°

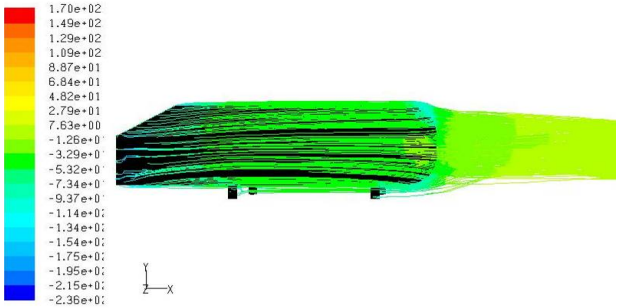

Vehicle model with θ = 30°

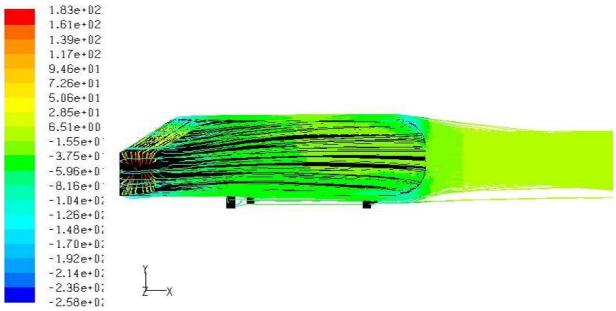

Vehicle model with θ = 35°

Figure 7. Pathlines colored by static pressure with blowing flow control

The presence of active control in the form of blowing was then evaluated based on the same parameter. Figure 7 presents contour pathlines colored by static pressure for models with the application of blowing active flow control for respective front slant angles. Figure 8 presents the distributions of pressure coefficients for given 16.7 m/s upstream velocity U_o as well as 0.5 m/s blowing velocity U_{bl}; all were applied on vehicle models with frontal slant angles of 25°, 30° and 35° respectively.

The figures show that with the application of blowing flow control, the pressure coefficient tends to increase. From around y/h=0.6 to y/h=1, pressure coefficients start to change in a positive direction. This finding shows that on the upper side of the rear part of respective model, pressure coefficient increases. By the application of blowing flow control, the lower pressure stream, and considering the shape factor and friction of air with model's wall can be reduced therefore the flow separation the rear part of the test model can be reduced as well. Table 3 summarizes the minimum values of the pressure coefficient distribution on a 0.5 m/s given blowing velocity U_{bl} and a 16.7 m/s upstream velocity U_o. The table also shows that the smallest pressure coefficient distribution was on the model with a 30° front slant angle when compared to the test model with 25° and 35° slant angles.

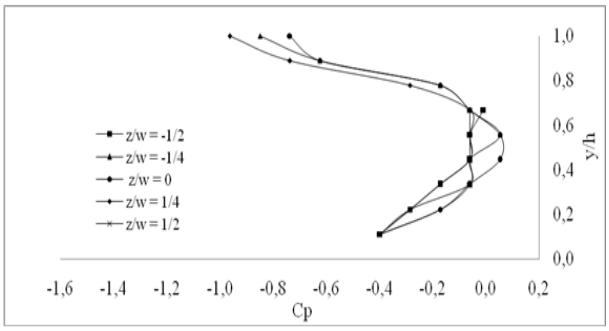

Vehicle model with θ = 25°

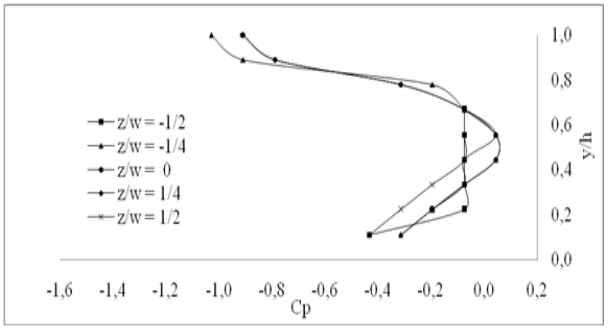

Vehicle model with θ = 30°

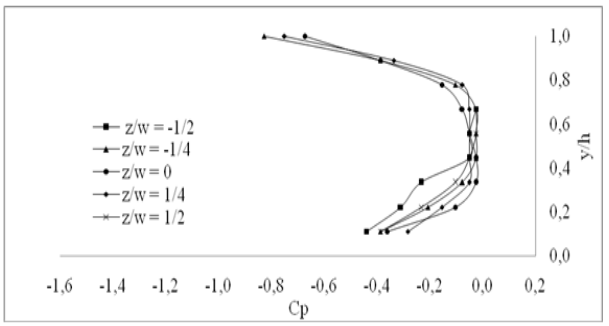

Vehicle model with θ = 35°

Figure 8. Pressure coefficient distribution with blowing flow control

Table 3. Minimum values of pressure coefficient with blowing flow control

Vehicle model	Pressure coefficient, C_p	y/h	z/w
$\theta=25^0$	-0.9622	1	1/4
$\theta=30^0$	-1.0285	1	-1/4
$\theta=35^0$	-0.8279	1	-1/4

The effect of additional active control by blowing with U_{bl}=0.5 m/s blowing speed in the reduction of the flow separation at the rear of each vehicle model is shown in table 4. The reduced flow separation gives an effect in the increase of the pressure coefficients on all vehicle models [33].

Table 4. Increasing pressure coefficient with blowing flow control

Vehicle model	Pressure coefficient, C_p		Increasing C_p, (%)
	Without active flow control	With blowing	
$\theta=25^0$	-1.1148	-0.9622	13.69
$\theta=30^0$	-1.0716	-1.0285	4.02
$\theta=35^0$	-1,3556	-0.8279	38.93

The largest value of increasing of pressure coefficient with the addition of blowing active control is on the model with 35° front slant angle gaining a number of percentages of 38.93%.

3.1 The computational method

Table 5 presented the aerodynamic drag coefficients for computational approach on the vehicle models with frontal slant angle of θ=25°, θ=30° and θ=35° both for normal treatment (without flow control) and with the addition blowing flow control with blowing speed U_{bl} of 0.5 m/s and upstream velocity U_o of 16.7 m/s.

Table 5. Aerodynamic drag coefficient and aerodynamic drag reduction by computational method

Vehicle model	Aerodynamic drag coefficient, C_d		Aerodynamic drag reduction, %
	without active flow control	with blowing	
$\theta=25^0$	1.7752	1.5639	11.90
$\theta=30^0$	1.6709	1.5699	6,04
$\theta=35^0$	1.7556	1.4953	14.81

Table 5 gives information that, in vehicle model without active control, the smallest aerodynamic drag coefficient is obtained in model with a 30° slant angle with the value of 1.6709 while on the models with 25° and 35° front slant angles, aerodynamic drag coefficients were 1.7752 and 1.7556 respectively. It is shown that the aerodynamic drag coefficients on each model were decreasing as the effect of the additional blowing active control while the smallest drag coefficient occurred in the model with θ=35°where the value of 1.4953. For models with θ=25° and θ=30°, the aerodynamic drag coefficients were 1.5639and 1.5699 respectively.

From the table 5 also, the largest reduction of aerodynamic drag as the effect of blowing flow control occurs on vehicle model with θ of 35° on a given 0.5 m/s blowing velocity U_{bl} and 16.7 m/s upstream velocity U_o with the reduction percentage was 14.81% . For the vehicle models with slant angles of 25°and 30°, the reduction were 11.90% and 6.04% respectively, as shown in table 5. The aerodynamic drag value on vehicle model with front slant angle 35° is capable to increase pressure coefficient on rear part of vehicle model for up to 38.93% as the effect of blowing flow control. The increasing of pressure coefficient on rear parts of vehicle models can decrease the aerodynamic drag. Results obtained from the research have confirmed the results of other researchers [16, 18, 23, 26, 27] where the application of active control by blowing can reduce aerodynamic drag on vehicle models.

3.2 The experimental method

Table 6 presents the aerodynamic drag coefficients obtained from experimental method on three vehicle models, which have similar geometric parameters to the model used for computational method.

Table 6 gives the information that for models without flow control, the smallest aerodynamic drag coefficients occurs in the 30° front slant angle vehicle model with 1.5173 value as for models with θ=25°and θ=35°,

the aerodynamic drag coefficients were 1.6237 and 1.5655 respectively. Additional blowing flow control for all models gives reduction of aerodynamic drag coefficients while the smallest aerodynamic drag coefficients occurred in the model with a 35°front slant angle with the value of 1.3747% and 1.4480% as well as 1.4313% for vehicle models with θ=25° and θ=30°.

Table 6. Aerodynamic drag coefficient and aerodynamic drag reduction by experimental method

Vehicle model	Aerodynamic drag coefficient, C_d		Aerodynamic drag reduction, %
	without active flow control	with blowing	
$\theta=25^0$	1.6237	1.4480	10.82
$\theta=30^0$	1.5173	1.4313	5.67
$\theta=35^0$	1.5655	1.3747	12.54

From the table 6 also, it is obvious that the smallest reduction of aerodynamic drag by active control with blowing speed U_{bl} of 0.5 m/s and upstream velocity U_o of 16.7 m/s occurred on the model with θ=35° giving the reduction of 12.54% while on models with θ=25° dan θ=30° the reductions were 10.82% and 5.67% respectively.

The comparison of aerodynamic drag coefficients for vehicle models with θ=25°, θ=30°and θ=35° front slant angles obtained from both computational method as well as experimental method are shown on tables 7, 8 and 9 respectively.

Table 7 contains the comparison of aerodynamic drag coefficient for vehicle model with slant angle θ=25° from computational and experimental methods. It is shown that the aerodynamic drags coefficients from the two methods on models without flow control differ in about 8.53%, as for models with a 0.5 m/s blowing flow control, the two methods result a 7.41% difference in the value of aerodynamic drag coefficient. The table 7 also informs that there is a 1.08% slight difference in the reduction of aerodynamic drag coefficient for the two methods.

Table 7. Aerodynamic drag coefficient (C_d) for vehicle model with $\theta=25^0$

Description	Aerodynamic drag coefficient, (C_d)		Aerodynamic drag coefficient (C_d) reduction (%)
	without active flow control	with blowing	
Computational	1.7752	1.5639	11.90
Experimental	1.6237	1.4480	10.82
Difference	8.53%	7.41%	1.08

Table 8 shows the comparison of aerodynamic drag coefficients from both computational and experimental approaches for vehicle model with slant angle of θ=30°.The coefficients of aerodynamic drag of the two methods for models without flow control differ on 9.19% differences. For vehicle models with blowing flow control at blowing speed of 0.5 m/s, the two methods give 8.83% difference in aerodynamic drag coefficient values. The table 8 also shows that the reduction of aerodynamic drag coefficients between computational and experimental methods differ on only 0.37%.

Table 8. Aerodynamic drag coefficient (C_d) for vehicle model with $\theta=30^0$

Description	Aerodynamic drag coefficient, (C_d)		Aerodynamic drag coefficient (C_d) reduction (%)
	without active flow control	with blowing	
Computational	1.6709	1.5699	6.04
Experimental	1.5173	1.4313	5.67
Difference	9.19%	8.83%	0.37

Table 9. Aerodynamic drag coefficient (Cd) for vehicle model with θ=350

Description	Aerodynamic drag coefficient, (C_d)		Aerodynamic drag coefficient (C_d) reduction (%)
	without active flow control	with blowing	
Computational	1.7556	1.4953	14.81
Experiment	1.5655	1.3706	12.54
Difference	10.82%	8.34%	2.27

Aerodynamic drag coefficients obtained from computational and experimental methods for θ=35° model are listed in table 9. For models without flow control, the aerodynamic drag coefficients of the two methods have 10.82% differences. On vehicle models with active blowing flow control at blowing speed of 0.5 m/s, the two methods give 8.34% difference in aerodynamic drag coefficient values. The table 9 also shows that the reductions of aerodynamic drag coefficients of the two methods differ about 2.27%.

4. CONCLUSION

Based on the results of pressure coefficients and drag reduction on reversed Ahmed vehicle models with front slant angles (θ) of 25°, 30° and 35° as well as the application of blowing flow control, some conclusion can be drawn. It is obvious that the active flow control by blowing and variations on front geometry provide significant impact to the increasing of pressure coefficients and reduction of aerodynamic drag. The most significant increase on pressure coefficients occurs on vehicle model with the 35° front slant angle, gaining 38.93% value, where pressure coefficients with and without blowing flow control reach -0.8279 and -1.3556, respectively. In terms of aerodynamic drag reduction, vehicle model with the 35° front slant angle also gains the value of 14.81 and 12.54 for computational and experimental methods, while the reductions of aerodynamic drag coefficients of the two approaches have 2.27% difference.

ACKNOWLEDGEMENTS

The research was funded by the Ministry of Research, Technology and Higher Education, The Republic of

Indonesia, through University Excellence Scheme F.Y 2018, with Research Contract No. : 1579/UN4.21/PL. 00.00/2018, dated March 21th 2018.

REFERENCES

[1] Agarwal, R.K."Sustainable ground transportation – review of technologies, challenges and opportunities", International Journal of Energy and Environment, Vol. 4, No.6, pp.1061-10782013, 2013.

[2] Ahmed, S., Ramm, G., Faltin, G."Some Salient Features Of The Time-Averaged Ground Vehicle Wake", SAE Technical Paper 840300, 1984.

[3] Sims-Williams, D., Dominy, R. "Experimental Investigation into Unsteadiness and Instability in Passenger Car Aerodynamics", SAE Technical Paper 980391, 1998.

[4] Bayraktar, I., Landman, D., Baysal, O. "Experimental and Computational Investigation of Ahmed Body for Ground Vehicle Aerodynamics", SAE Technical Paper 2001-01-2742, 2001.

[5] Joseph, P., Amandolese, X., Edouard, C. Aider, J. "Flow control using MEMS pulsed micro-jets on the Ahmed body", Experiment in Fluids, Vol. 54, No. 1, 1442, 2013.

[6] Lienhart, H., Becker, S. "Flow and Turbulence Structure in the Wake of a Simplified Car Model", SAE Technical Paper 2003-01-0656, 2003,

[7] Han, T. "Computational analysis of three-dimensional turbulent flow around a bluff body in ground proximity", AIAA Journal, Vol. 27, No.9, 1989, pp. 1213-1219.

[8] Basara, B., Przulj, V., Tibaut, P. "On the Calculation of External Aerodynamics: Industrial Benchmarks", SAE Technical Paper 2001-01-0701, 2001.

[9] Basara, B. "Numerical simulation of turbulent wakes around a vehicle", in: *ASME Fluid Engineering Division Summer Meeting FEDSM99-7324*. San Francisco, USA, 1999.

[10] Basara, B., Alajbegovic, A. "Steady state calculations of turbulent flow around Morel body". in: *7th International Symposium of Flow Modelling and Turbulence Measurements*, Taiwan, 1998, pp. 1–8

[11] Gilliéron, P.,Chometon, F. "Modeling of stationary three-dimensional separated air flows around an Ahmed reference model", in : *ESAIM, Proceeding of Third International Workshop on Vortex Flows and Related Numerical Methods*, 7, 1999, pp. 173–182.

[12] Kapadia, S., Roy, S., Vallero, M., Wurtzler, K., Forsythe J. "Detached-Eddy Simulation over a Reference Ahmed Car Model", in: Friedrich, R., Geurts, B.J., Métais, O. (eds*) Direct and Large-Eddy Simulation V*. ERCOFTAC Series, 9. Springer, Dordrecht, 2004, pp 481-488.

[13] Conan, B., Anthoine, J., Planquart, P. "Experimental aerodynamic study of a car-type bluff body", Experiments in Fluids, Vol. 50, No. 5, pp.1273-1284, 2010.

[14] Krogstad, P.A., Kourakine, A. "Some effects of localized injection on the turbulence structure in a boundary layer", Physics of Fluids, Vol. 12, No.11, pp. 2990-2999, 2000.

[15] Park, J., Choi, H. "Effects of uniform blowing through blowing or suction from a spanwise slot on a turbulent boundary layer flow", Physics of Fluids, Vol. 11, No. 10, pp. 3095–3105, 1999.

[16] Krentel D., Muminovic R., Brunn A., Nitsche W., King R. "Application of Active Flow Control on Generic 3D Car Models". in: King R. (eds) *Active Flow Control II. Notes on Numerical Fluid Mechanics and Multidisciplinary Design*, 108. Springer, Berlin-Heidelberg, Germany, 2010, pp. 223-239.

[17] Heinemann, T., Springer, M., Lienhart, H. "Active flow control on a 1:4 car model", Experiments in Fluids, Vol. 55, No. 5, 1738, 2014.

[18] Mestiri, R., Ahmed-Bensoltane, A., Keirsbulck, L., Aloui, F.,Labraga, L. "Active Flow Control at the Rear End of a Generic Car Model Using Steady Blowing", Journal of Applied Fluid Mechanics, Vol. 7, No. 4, pp. 565-571, 2014.

[19] Tounsi, N., Mestiri, R., Keirsbulck, L., Oualli, H., Hanchi, S., Aloui, F."Experimental Study of Flow Control on Bluff Body using Piezoelectric Actuators" , Journal of Applied Fluid Mechanics , Vol. 9, No. 2, pp. 827-838, 2016.

[20] Tian, J., Zhang, Y., Zhu, H., Xiao, H."Aerodynamic drag reduction and flow control of Ahmed body with flaps", Advances in Mechanical Engineering, Vol. 9, No.7, pp. 1–17, 2017.

[21] Shadmani, S., Mousavi-Nainiyan, S.M., Ghasemiasl, R.,Mirzaei, M., Pouryoussefi, S.G. "Experimental Study of Flow Control Over an Ahmed Body Using Plasma Actuator", Mechanics and Mechanical Engineering, Vol. 22, No. 1, pp. 239–251, 2018.

[22] Prakash, B., Bergada, J.M., Mellibovsky, F. "Three Dimensional Analysis of Ahmed Body Aerodynamic Performance Enhancement using Steady Suction and Blowing Flow Control Techniques", in : *Tenth International Conference on Computational Fluid Dynamics (ICCFD10)*, 2018. Barcelona, Spain.

[23] Harinaldi, Budiarso, Tarakka, R., Simanungkalit, S.P. "Effect of Active Control by Blowing to Aerodynamic Drag of Bluff Body Van Model", International Journal of Fluid Mechanics Research, Vol. 40, No.4, pp. 312-323, 2013.

[24] Julian, J., Karim, R.F., Budiarso, Harinaldi, "Review: Flow Control on a Squareback Model" International Review of Aerospace Engineering (IREASE), Vol. 10, No. 4, pp. 230-239, 2017.

[25] Harinaldi, Budiarso, Warjito, Kosasih, E.A., Tarakka, R., Simanungkalit, S.P. "Active technique by suction to control the flowstructure over a van model", Journal of Engineering and Applied Science, Vol. 7, No. 2, pp.215-222, 2012.

[26] Harinaldi, Budiarso, Tarakka, R., Simanungkalit, S.P. "Computational Analysis of Active Flow Control to Reduce Aerodynamics Drag on a Van Model", International Journal of Mechanical & Mechatronics Engineering IJMME-IJENS, Vol. 11, No. 3, pp. 24-30, 2011

[27] Tarakka, R., Jalaluddin, Mire, B., Umar, M.N. "Effect of Turbulence Model In Computational Analysis of Active Flow Control on Aerodynamic Drag of Bluff Body Van Model", International Journal of Applied Engineering Research, Vol. 10, No. 1, pp. 207-219, 2015.

[28] Tarakka, R., Salam, N., Jalaluddin, Ihsan, M. "Active Flow Control by Suction on Vehicle Models with Variations on Front Geometry", International Review of Mechanical Engineering, Vol. 12, No. 2, 2018, pp. 128-134.

[29] Plint and Partners, Manual of Educational Wind Tunnel, England, 1982.

[30] Ocokoljić, G., Damljanović, D., Vuković, Đ., Rašuo, B. "Contemporary Frame of Measurement and Assessment of Wind-Tunnel Flow Quality in a Low-Speed Facility", FME Transactions, Vol. 46, No. 4, pp. 429-442, 2018.

[31] Ocokoljić, G., Damljanović, D., Rašuo, B., Isaković, J. "Testing of a Standard Model in the VTI's Large subsonic Wind-tunnel Facility to Establish Users' Confidence", FME Transactions, Vol. 42, No. 3, pp. 212-218, 2014.

[32] Anderson, J.D. "Fundamental of Aerodynamics" 3rd ed., McGraw-Hill, Singapore, 2001.

[33] Sphon, A., Gilliéron, P. "Flow separations generated by simplified geometry of an automotive vehicle", in: *IUTAM Symposium: Unsteady separated flows*, 2002, Toulouse, France.

NOMENCLATURE

Cd	drag coefficient
Cp	pressure coefficient
Fd	pressure drag force [N]
h	height of test model [m]
l	length of test model [m]
ρ	density [kg/m^3]
θ	front slant angle [^{o}]
Re	Reynolds number
S	cross section area [m^2]
τ_w	wall shear stress [N/m^2]
U_{bl}	blowing velocity [m/s]
U_o	upstream velocity [m/s]
μ	viscosity [N.s/m^2]
w	width of test model [m]

УТИЦАЈ РЕГУЛАЦИЈЕ ПРОТОКА ДУВАЊА И ПРЕДЊЕ ГЕОМЕТРИЈЕ НА СМАЊЕЊЕ АЕРОДИНАМИЧКОГ ОТПОРА КОД МОДЕЛА ВОЗИЛА

Р.Тарака, Н.Салам, Џалалудин, М.Ихсан

Анализира се утицај регулације протока дувања и варијације предње геометрије у циљу редукције аеродинамичког отпора код модела возила. Регулација протока дувања је алтернативна мера за модификацију почетка раздвајања протока у граничном слоју на површини возила. Очекује се да се модификацијом смањи доминантан утицај области раздвајања на укупан отпор. Истраживање извршено нумеричким и експерименталним методама се бави испитивањем утицаја варијација предњег нагибног угла од 25^0, 30^0 и 35^0 на редукцију аеродинамичког отпора код модела возила при регулацији протока дувања узлазно и брзине протока од 16,7 м/с односно 0,5 м/с. Мерне ћелије су коришћене код експеримента за евалуацију аеродинамичког отпора израчунатог нумеричком методом. Утврђено је да регулација протока дувања и варијације предње геометрије имају значајан утицај на повећање коефицијената притиска и смањење аеродинамичког отпора код модела возила. Највеће повећање коефицијената притиска од 38,93% је било код модела са нагибним углом од 35^0, док је највеће смањење аеродинамичког отпора било на истом моделу: од 14,81 – 12,54 применом нумеричке односно експерименталне методе.